Am J Physiol Regul Integr Comp Physiol 300: R1100–R1114, 2011.
First published February 9, 2011; doi:10.1152/ajpregu.00653.2010.

Elevated seawater P_{CO_2} differentially affects branchial acid-base transporters over the course of development in the cephalopod *Sepia officinalis*

Marian Y. Hu,[1] Yung-Che Tseng,[2] Meike Stumpp,[1] Magdalena A. Gutowska,[3] Rainer Kiko,[1] Magnus Lucassen,[4] and Frank Melzner[1]

[1]*Biological Oceanography, Leibniz-Institute of Marine Sciences (IFM-GEOMAR), Kiel, Germany;* [2]*Institute of Cellular and Organismic Biology, Academia Sinica, Nankang, Taipei, Taiwan, Republic of China;* [3]*Institute of Physiology, Christian-Albrechts-University, Kiel, Germany; and* [4]*Alfred Wegener Institute for Polar and Marine Research, Bremerhaven, Germany*

Submitted 4 October 2010; accepted in final form 9 February 2011

Hu MY, Tseng YC, Stumpp M, Gutowska MA, Kiko R, Lucassen M, Melzner F. Elevated seawater P_{CO_2} differentially affects branchial acid-base transporters over the course of development in the cephalopod *Sepia officinalis. Am J Physiol Regul Integr Comp Physiol* 300: R1100–R1114, 2011. First published February 9, 2011; doi:10.1152/ajpregu.00653.2010.—The specific transporters involved in maintenance of blood pH homeostasis in cephalopod molluscs have not been identified to date. Using in situ hybridization and immunohistochemical methods, we demonstrate that Na^+/K^+-ATPase (*soNKA*), a V-type H^+-ATPase (*soV-HA*), and Na^+/HCO_3^- cotransporter (*soNBC*) are colocalized in NKA-rich cells in the gills of *Sepia officinalis*. mRNA expression patterns of these transporters and selected metabolic genes were examined in response to moderately elevated seawater P_{CO_2} (0.16 and 0.35 kPa) over a time course of 6 wk in different ontogenetic stages. The applied CO_2 concentrations are relevant for ocean acidification scenarios projected for the coming decades. We determined strong expression changes in late-stage embryos and hatchlings, with one to three log2-fold reductions in *soNKA*, *soNBCe*, *socCAII*, and *COX*. In contrast, no hypercapnia-induced changes in mRNA expression were observed in juveniles during both short- and long-term exposure. However, a transiently increased ion regulatory demand was evident during the initial acclimation reaction to elevated seawater P_{CO_2}. Gill Na^+/K^+-ATPase activity and protein concentration were increased by ~15% during short (2–11 days) but not long-term (42-days) exposure. Our findings support the hypothesis that the energy budget of adult cephalopods is not significantly compromised during long-term exposure to moderate environmental hypercapnia. However, the downregulation of ion regulatory and metabolic genes in late-stage embryos, taken together with a significant reduction in somatic growth, indicates that cephalopod early life stages are challenged by elevated seawater P_{CO_2}.

acid-base regulation; Na^+/K^+-ATPase; SLC4 family; embryonic development; ocean acidification

WATER-BREATHING ECTOTHERMIC animals maintain a diffusion gradient of CO_2 across respiratory epithelia to excrete this metabolic end product. Increases in seawater P_{CO_2} (hypercapnia) lead to an increased P_{CO_2} of body fluids to maintain the diffusive flux of CO_2 out of the animal (63). Environmental hypercapnia is a stressor that has lately received considerable attention: anthropogenic CO_2 emissions are expected to lead to increases in surface ocean P_{CO_2} from 0.04 kPa up to 0.14 kPa (ocean acidification) within this century (6). However, a high variability of abiotic factors is the rule in many coastal habitats already (47), and hypercapnia is a characteristic of many marine systems, e.g., in upwelling regions along the continental shelfs (27) and seasonally hypoxic systems (80). It can be expected that effects of ocean acidification will increase P_{CO_2} in a nonlinear fashion in coastal CO_2-enriched habitats, probably leading to P_{CO_2} values ~0.2 to 0.4 kPa within the next decades (80).

Physiological tolerance to elevated seawater P_{CO_2} is hypothesized to be connected to the ability of an organism to regulate extracellular acid-base status during exposure to hypercapnia, especially in organisms that rely on pH-sensitive respiratory pigments (73). Accordingly, active marine ectotherms (i.e., teleosts, crustaceans, cephalopods) have been found to be the most tolerant to environmental hypercapnia as their high metabolic rates are supported by efficient acid-base regulation (64). This compensatory reaction has been studied in great detail in teleost fish (e.g., 12, 13, 52, 81), where extracellular pH (pHe) is fully compensated during hypercapnia by net accumulation of bicarbonate (HCO_3^-) via ion transporting of cells of the gill epithelium. For example, in response to a P_{CO_2} of 1 kPa, cod *Gadus morhua* compensate extracellular acidosis by actively increasing blood HCO_3^- concentration ($[HCO_3^-]$) from 10 to 30 mM accompanied by an equimolar reduction in plasma chloride concentrations (58, 81). Only decapod crustaceans have been shown to posses comparable acid-base regulatory abilities (7, 68, 79). Recently, Gutowska et al. (41) demonstrated that a cephalopod, *Sepia officinalis*, can also efficiently maintain high pHe when exposed to hypercapnia (0.6 kPa) by increasing blood $[HCO_3^-]$ from 3.4 to 10.4 mM. However, the mechanisms that contribute to pHe regulation in cephalopods are unexplored at present.

Acid-base regulating epithelia and organs have been extensively investigated in a number of marine fish species (15, 23, 39, 51, 63, 77). These studies proposed models of acid-base regulation in specialized, mitochondria-rich cells localized in skin or gill epithelia. Besides the direct ATP-dependent extrusion of protons via V-type H^+-ATPases, these models suggest an import of HCO_3^- and an export of protons by secondary active transporters, e.g., apical Na^+/H^+ exchangers (NHE) and Na^+-dependent Cl^-/HCO_3^- exchangers of the SLC4 solute transporter family that depend on the electrochemical gradient created by the Na^+/K^+-ATPase (NKA) located in basolateral membranes (4, 23, 48, 70). In cephalopods, little is known on the specific transporters involved in branchial acid-base regulation. Earlier studies have demonstrated that NKA also occurs in basolateral membranes of cephalopod gills with maximum activity levels comparable to those described for shallow-water

Address for reprint requests and other correspondence: M. Y. Hu, Biological Oceanography, Leibniz-Institute of Marine Sciences (IFM-GEOMAR), Kiel 24105, Germany (e-mail: mhu@ifm-geomar.de).

 0363-6119/11 Copyright © 2011 the American Physiological Society

teleost fish (33, 49, 75, 84). In contrast to the fish gill, the gill of the decapod cephalopod *S. officinalis* (cuttlefish) is a highly folded epithelium consisting of two epithelial layers that line a blood sinus. The thin peripheral layer has been hypothesized to be primarily involved in respiration, whereas the inner epithelium is responsible for ion regulation and, probably, nitrogen excretion (19, 75). Immunohistochemical and cytochemical findings suggest an analogy between cells of this inner epithelium and ionocytes of teleosts and their capacity for active ion transport (49, 75). In this inner, mitochondria-rich epithelium, Schipp et al. (75) demonstrated the presence of cytoplasmatic carbonic anhydrase (cCA), as well as several dehydrogenases (malate-, succinate-, and glucose-6-phosphate dehydrogenase) that are involved in aerobic metabolism. Furthermore, Schipp et al. (75) described that the gill epithelium is not fully developed in late-stage embryos, with significant differentiation occurring posthatching. This could imply that cuttlefish embryos and young hatchlings have significantly weaker ion regulatory capacities than juveniles or adults, especially if no alternative sites, such as skin integument or yolk epithelium cover these functions.

Yet, late-stage cephalopod embryos are exposed to stressful abiotic conditions inside the egg capsule: *1*) P_{O_2} can be as low as 5 kPa and *2*) P_{CO_2} can reach values of up to 0.4 kPa (14, 40). This is due to the egg capsule wall acting as a diffusion barrier to dissolved gases. The transition phase from the hypoxic and hypercapnic environment of the egg fluid to seawater is an extraordinary event in the life history of cephalopods. Not only do abiotic conditions dramatically change, but the metabolic rates of the hatchlings also steeply increases (e.g., 14). Both significantly challenge the maintenance of acid-base homeostasis and require potent acid-base regulatory machinery.

This is the first study to examine mechanisms of hypercapnia induced acid-base regulation in cephalopods on the molecular level. In a first step, we used information on acid-base regulation in fish as a guide to clone putative acid-base regulation genes of the cuttlefish gill, encoding for NKA (*soNKA*), cCA (*socCAII*), and V-type-H^+-ATPase (*soV-HA*) plus two HCO_3^- transporters, electrogenic Na^+/HCO_3^- cotransporter (*soNBCe*) and Na^+ dependent Cl^-/HCO_3^- exchanger (*soNDCBE*). We then studied transcriptional responses of acid-base and selected metabolic genes (*soNKA*, *soCAII*, *soNBCe*, *soNDCBE*, ATP-synthase, octopine dehydrogenase, cytochrome-*c* oxydase, and cytochrome *P*-450) in different life stages of the cuttlefish *S. officinalis*. We hypothesized that in response to hypercapnia, acid-base regulatory gene candidate transcripts would show specific upregulations to support an increased demand of the acid-base regulating machinery and that the elevated metabolic requirements for acid-base regulation would be reflected in an upregulation of marker genes for key metabolic pathways. Functional capacities of NKA were determined, as this enzyme is believed to be the major driving force for most energy-dependent ion transport. We further hypothesized that increases in environmental P_{CO_2} as projected by ocean acidification scenarios must be additive to the P_{CO_2} inside the egg to maintain a sufficient diffusion gradient of CO_2 from the egg to the seawater. This extreme egg environment and the incompletely developed ion regulatory epithelia of embryos would then lead to a higher sensitivity of embryonic life stages toward acid-base disturbances.

MATERIAL AND METHODS

Experimental Animals

S. officinalis egg clusters were collected in Zeeland, Netherlands, in May 2008 and 2009 and transported to the Leibniz-Institute of Marine Sciences (IFM-GEOMAR), Kiel, at stage 17–20 [stages according to Lemaire (59)]. After hatching, cuttlefish were raised in a closed recirculating system (1,200-liter total volume; protein skimmer; nitrification filter; UV disinfection unit; salinity, 31–32; NH_4^+, <0.1 mg/l; NO_2^-, <0.1 mg/l, NO_3^-, <10 mg/l; temperature, 15°C; and constant 12:12-h dark-light cycle). Cuttlefish hatchlings were initially fed with live mysids and were progressively transitioned to feed on *Paleamonetes varians.* The animals displayed normal development and behavior.

CO_2 Pertubation Experiments

Experiment 1: embryos and hatchlings. S. officinalis egg clusters were collected in May 2009. Then 25 to 30 individual eggs containing embryos [stage 17–18 (60)] were incubated in nine PVC aquaria (25-liter volume) inside a 15°C climate chamber for 8 wk. The aquaria were continuously equilibrated with the appropriate gas mixtures (0.04 kPa, 0.14 kPa, and 0.4 kPa CO_2 in pressurized air) supplied by a central automatic gas mixing-facility (Linde Gas, HTK Hamburg, Germany). The nine tanks, with three replicate tanks for each treatment, were randomly distributed in a water bath. A light regimen with a 12:12-h light-dark cycle was chosen. Artificial seawater (SEEQUASAL, Münster, Germany) was prepared in three 400-liter reservoir tanks and preequilibrated with the respective P_{CO_2}. Two thirds of the water in the experimental tanks were exchanged daily with CO_2 preequilibrated water from the reservoir tanks to maintain high water quality within the system. For sampling of gill tissues, late-stage embryos [stage 30 (59)] and hatchlings (2 days posthatching) were dissected by opening of the ventral mantle cavity. The two gills, which were ~1.5 mm in length, were quickly dissected with two sharp forceps, shock frozen in liquid nitrogen, and stored at −80°C for gene expression analysis.

Determination of Perivitelline Fluid Abiotic Parameters

At the final stage of development [stage 30 (59)] eggs were carefully lifted out of the water, and the perivitelline fluid (PVF) was immediately sampled from the egg by using a syringe. A pH electrode (models WTW Mic and pH340i pH meter; WTW, Weilheim, Germany), calibrated with seawater AMP and Tris buffers (18), was used to measure PVF pH in 0.5-ml Eppendorf tubes. Another 500 μl of PVF was sampled with a gas-tight glass syringe for the determination of total dissolved inorganic carbon (C_T). C_T was measured in triplicate (100 μl each) using a Corning 965 carbon dioxide analyzer (Olympic Analytical Service, Malvern, UK). The carbonate system speciation was calculated from C_T and pH NBS scale (pH_{NBS}) with the CO2SYS software and using the dissociation constants of Mehrbach et al. (62) as refitted by Dickson and Millero (16). During the measurement period for pH and P_{O_2}, the PVF sample and sensors were placed in a thermostatted water bath at 15°C. The oxygen optode was calibrated according to the manufacturer's instructions with water vapor-saturated air and a Na_2SO_3 solution. Following PVF sampling, eggs were dissected and biometric parameters were determined. Body dimensions, including dorsal mantle length (DML) and body mass were determined using a Leica MZ95 stereo microscope equipped with a closed caption device (CCD) camera and using Image-Pro Plus software (Media Cybernetics, Bethesda, MD). Animal wet mass was determined by using a precision balance (Sartorius TE64). In total, 15 eggs were sampled for each treatment.

Experiment 2: juveniles. Forty-eight *S. officinalis* specimen (DML, 3–4 cm) were maintained in a flow-through seawater system consisting of 16 PVC aquaria (25-liter volume) in a 15°C climate chamber at the IFM-GEOMAR, Kiel. A light regimen with a 12:12-h light-dark

cycle was chosen. Artificial seawater was prepared daily in a 400-liter reservoir tank. From this reservoir tank the water passed through a 12-W UV sterilizer before being distributed to the experimental aquaria via gravity feed at a rate of 20 m/min. Before the start of the experiments the animals were maintained under control conditions for 14 days. The experimental tanks contained three individuals. Tanks were continuously equilibrated with the appropriate gas mixture (0.3 kPa CO_2) supplied by the central automatic gas mixing-facility or pressurized air (0.04 kPa) and randomly arranged with respect to CO_2 level. Throughout the duration of the experiment, cuttlefish were fed daily with one live *P. varians* each (~10–15% of cuttlefish body mass). It needs to be noted that juveniles were not fed ad libitum, but food supply was high enough to produce growth rates of 1.5% per day, which relates to maximum growth rates of 4% observed for animals of comparable size and at the same temperature (e.g., 30, 37).

Tissue samples were taken 2, 11, and 42 days after the start of the experiment. At each time point, eight specimens from each treatment (total of 16 animals, one from each of 8 replicate aquaria) were anaesthetized in 2.5% EtOH in seawater for ~2–3 min. Afterward the animals were killed by decapitation, and the mantle cavity was opened on the ventral side. The gills were immediately dissected using micro scissors and forceps. The tip of the left gill was fixed with 4% paraformaldehyde in seawater at 4°C overnight and then washed several times with PBS. These gills were stored in 100% MeOH at −80°C for in situ hybridization. The remaining right and left gill were quickly shock-frozen in liquid nitrogen and stored at −80°C for enzyme assays and gene expression analysis. The investigations comply with the German animal welfare principles No. V 31, and the animal use protocols were approved by the animal care committee of the Christian-Albrechts-University, Kiel, Germany.

Determination of Seawater Abiotic Parameters

Specific seawater conditions for the various incubations are given in Table 1. Temperature, pH_{NBS}, and salinity were determined daily. pH_{NBS} was measured with a WTW 340i meter and WTW SenTix 81 electrode calibrated daily with Radiometer IUPAC precision pH_{NBS} buffers 7.00 and 10.00 (S11M44, S11 M007). Additionally, water ammonia concentrations were determined every 2 to 3 days, and levels were maintained < 0.3 mg/l.

C_T was measured coulometrically according to Dickson et al. (18) by using a Single-Operator Multi-Metabolic Analyzer auto analyzer (Marianda, Kiel, Germany). Total alkalinity (A_T) was determined by using the methods of Dickson et al. (18) by means of a potentiometric open-cell titration with hydrochloric acid. The measurement was performed using a Versatile Instrument for the Determination of Titration Alkalinity auto analyzer (Marianda). As reference material for both types of analysis (C_T as well as A_T) certified reference material was used (17). Seawater carbonate chemistry speciation was calculated from C_T and A_T with the software CO2SYS (60) using the dissociation constants of Mehrbach et al. (62) as refitted by Dickson and Millero (16).

Cloning of soNKA, soNBCe, soNDCBE, socCAII, and soV-AH Fragments

Fragments of the *Sepia* NKA (*NKA*), Na^+/HCO_3^- co-transporter (*NBC*), Na^+-dependent Cl^-/HCO_3^- exchanger (*NDCBE*), cCA (*CA*), and V-type-ATPase (*V-HA*) genes were isolated from gill tissue by means of RT followed by PCR. Degenerate primers were designed using MacVector 10.0.2 (Symantec) software, by using highly conserved regions of sequences of cephalopods, bivalves, and fish obtained from GenBank. Reverse transcription was performed with Superscript RT (Invitrogen, Karlsruhe, Germany) and gene-specific primers according to the manufacturer's instructions with mRNA as templates (see next section for RNA extraction protocol). In the following PCR, primer pair 5′-AAGTCGTGCCAATGTGTTGTA-3′ and 5′-TACTTYCCACGWGGACTTTCTTAG-3′ resulted in a 268-bp fragment of the *NKA* (GQ153672.1), the primer pair 5′-GCGGAAGGAGGTGTAGAAGAAGT-3′ and 5′-CATAGTCHAGTGTCGTAAGTAGGC-3′ resulted in a 582-bp fragment of *NBC* (bankit1344341), the primer pair 5′-GCCAGRTGGATWAAGTTTGA-3′ and 5′-GGTWGGSACRGGRACCTCTG-3′ resulted in a 693-bp fragment of the *NDCBE* (bankit1344354), the primer pair 5′-CTACARYTAYCCYCTRACCGC-3′ and 5′-AAAGTRAARGTGACCCCKAG-3′ resulted in a 215-bp fragment of cytosolic *CAII* (bankit1344380), and the primer pair 5′-GARTAYTTYMGNGAYATGGGN-3′ and 5′- RTTYTGYTGNARRAARTCRTCYTT-3′ resulted in a 556-bp fragment of *VHA* subunit a (bankit1370003). The sequences obtained for cytosolic CAII and NBCe of cuttlefish show high similarities compared with teleosts and mammals (Supplemental Fig. S2).

cDNA was amplified using Taq-Polymerase (Invitrogen, Karlsruhe, Germany) in the presence of 1.5 mM $MgCl_2$ (PCR conditions: 4-min denaturation at 94°C, 45-s annealing at 53°C and 45-s elongation at 72°C, 35 cycles followed by a final amplification step of 8 min at 72°C). PCR fragments were separated after electrophoresis in 1% agarose gels. Extraction and purification of the PCR fragments from the gel was accomplished using the QIAquick gel extraction kit (Qiagen, Hilden, Germany). Cloning and isolation of plasmids was performed using the pGEM-T Easy Vector Systems and JM 109 competent *Escherichia coli* cells (Promega, Madison, WI). Plasmids were extracted using the Qiaprep Spin Miniprep Kit (Qiagen) and sequenced by the sequencing platform of the Institute for Clinical Molecular Biology (IKMB), Christian-Albrechts-University of Kiel (Kiel, Germany).

Real-Time Quantitative PCR

For RNA extraction, whole gills from embryos, hatchlings, and juveniles were homogenized under liquid nitrogen, using pestle and mortar. Homogenates (25 mg) were used for further extraction. RNA extraction was performed according to the manufacturer's instructions with an additional cleaning step using the QIAshredder column (Qiagen) performed after homogenization in RNeasy lysis buffer. RNA was eluted and stored in 100 μl RNase-free water at −80°C. DNA contaminations were removed by DNase digestion with the DNA-free kit (Applied Biosystems, Darmstadt, Germany). Concentration and integrity of the isolated RNA was determined photometrically using a NanoDrop ND-1000 spectrophotometer (PeqlabEQLAB, Erlangen, Germany) and via electrophoresis using the Experion electrophoresis system (Bio-Rad, Munich, Germany).

Primers for quantitative real-time PCR (qRT-PCR) were designed using the primer analysis software Primer Express version 2.0 (Applied Biosystems) with the default parameters of the TaqMan MGB Probe and Primer design procedure. We selected PCR amplicons to

Table 1. *Seawater physiochemical conditions during 6-wk hypercapnia experiment (juvenile S. officinalis)*

	Incubation Group	Temperature, °C	Salinity	pH	ΩAr	P_{CO_2}, Pa	A_T
Embryos and hatchlings	control	14.60 ± 0.47	34.94 ± 0.10	7.96 ± 0.02	1.69 ± 0.06	70.97 ± 4.13	2,413.81 ± 49.10
	P_{CO_2} ~0.14 kPa	14.62 ± 0.47	34.92 ± 0.07	7.63 ± 0.02	0.84 ± 0.01	164.04 ± 24.48	2,431.89 ± 56.12
	P_{CO_2} ~0.4 kPa	14.62 ± 0.45	34.90 ± 0.05	7.28 ± 0.03	0.39 ± 0.02	371.35 ± 28.52	2,415.16 ± 43.00
Juveniles	control	14.81 ± 0.20	33.08 ± 0.20	8.21 ± 0.08	3.53 ± 0.53	50.255 ± 8.757	2,827.00 ± 129.08
	P_{CO_2} ~0.4 kPa	14.83 ± 0.21	33.09 ± 0.21	7.39 ± 0.09	0.75 ± 0.11	308.936 ± 37.401	3,127.53 ± 141.91

Values are presented as means ± SD. P_{CO_2}, partial pressures of CO_2; Ω_{Arag}, aragonite saturation state; A_T, total alkalinity.

range from 50 to 100 bp in size. Selected genes and primer sequences are given in Table 2. ATP-Synthase, cytochrome *P*-450, ubiquitin-conjugated enzyme and cleavage and polyadenylation specificity factor sequences were obtained from an *S. officinalis* gill cDNA library (F. Melzner, R. Kiko, M. Lucassen, unpublished observation). qRT-PCR was performed on an ABI StepOne Plus Sequence Detection System (Applied Biosystems) using the Power SYBR Green QPCR Master Mix (Applied Biosystems). The PCR reaction consisted of 10 μl SYBR Green PCR master mix, 3 μl (2 pmol/μl) forward and reverse primers, 2.0 μl 1:10-diluted template cDNA and 2.0 μl water in a total reaction volume of 20 μl. Thermocycling was performed using the following conditions: 10 min at 95°C, 45 cycles of 15 s at 95°C, and 1 min at 62°C. Melting curve analysis demonstrated a single PCR amplicon for each reaction. Data were recorded as fractional cycle at an arbitrary C_T-value in triplicate during the exponential phase of the reaction. To determine the amplification efficiency of each primer pair, a standard curve of four serial dilution points (in steps of 2-fold) of a cDNA mixture was analyzed using linear regression. The amplification efficiency of an individual reaction was determined using the ABI StepOne Plus Sequence Detection System. PCR efficiencies of investigated genes ranged from 1.84 to 2.0.

NormFinder, a Microsoft Excel add-in (available at http://www.mdl.dk/publicationsnormfinder.htm) was used to identify housekeeping gene candidates. The genes cleavage and polyadenylation specificity factor (*CPSF*) and ubiquitin conjugated protein (*UBC*) were identified as the best housekeeping genes between treatments and incubation times. For the normalization factor (NF_n) the geometric mean of the best fitting housekeepers ($REF_{1\text{-}n}$) was calculated.

NKA Activity Assay

NKA activity was measured in gill tissue crude extracts of juvenile specimens in a coupled enzyme assay with pyruvate kinase (PK) and lactate dehydrogenase (LDH) using the method of Schwarz et al. (76) as described by Melzner et al. (63). Crude extracts were obtained by quickly homogenizing the tissue samples in a conical tissue grinder in 10 volumes of ice-cold buffer [50 mM imidazole, pH 7.8, 250 mM sucrose, 1 mM EDTA, 5 mM β-mercaptoethanol, 0.1% (wt/vol) deoxycholate, proteinase inhibitor cocktail (cat. no. P8340; Sigma-Aldrich Taufkirchen, Germany)] followed by Ultra Turrax treatment (3× 5 s) on ice. Cell debris was removed by centrifugation for 10 min at 1,000 *g* and 4°C. The supernatant was used as crude extract. The reaction was started by adding 10 μl of the sample homogenate to the reaction buffer containing 100 mM imidazole, pH 7.8, 80 mM NaCl, 20 mM KCl, 5 mM $MgCl_2$, 5 mM ATP, 0.24 mM Na-($NADH_2$), 2 mM phosphoenolpyruvate, ~12 U/ml PK and 17 U/ml LDH, using a PK/LDH enzyme mix (Sigma-Aldrich). The oxidation of NADH coupled to the hydrolysis of ATP was followed photometrically at 15°C in a DU 650 spectrophotometer (Beckman Coulter) over a period of 10 min, measuring the decrease of extinction at $\lambda = 339$ nm. The fraction of NKA activity in total ATPase activity was determined by the addition of 17 μl of 5 mM ouabain to the assay. Each sample ($n = 8$) was measured sextuple. Enzyme activity was calculated using an extinction coefficient for NADH of $\varepsilon = 6.31$ mM/cm and given as micromoles ATP per gram per hour.

Immunoblotting

For immunoblotting, 20 μl of crude extracts from the NKA activity measurement were used. Proteins were fractionated by SDS-PAGE on 10% polyacrylamide gels, according to Lämmli (57) and transferred to PVDF membranes (Bio-Radmany) using a tank blotting system (Bio-Rad). Blots were preincubated for 1 h at room temperature in TBS-Tween buffer [TBS-T, 50 mM Tris·HCl, pH 7.4, 0.9% (wt/vol) NaCl, 0.1% (vol/vol) Tween20] containing 5% (wt/vol) nonfat skimmed milk powder. The primary antibody for the NKA was the polyclonal antibody α (H-300) (Santa Cruz Biotechnology, Heidelberg, Germany) specific to the *S. officinalis* α-subunit of the NKA (49). Blots were incubated with primary antibodies with a concentration of 2 μg/ml at 4°C overnight. After washing with TBS-T, blots were incubated for 1 h with horseradish peroxidase-conjugated goat anti-rabbit IgG antibody(Santa Cruz Biotechnology, Santa Cruz, CA) diluted 1:2,000 in TBS-T containing 5% nonfat skimmed milk powder. Protein signals were visualized by using the ECL Western Blotting Detection Reagents (GE Healthcare, Munich, Germany) and recorded using a LAS-1000 CCD camera (Fuji, Tokyo, Japan). Signal intensity was calculated using the AIDA Image Analyzer software (version 3.52; Raytest, Straubenhardt, Germany).

Table 2. *Primer sequences used for qRT-PCR*

Gene	Abbreviation	Function	Acc. No.	Primer Sequence 5′-3′ (forward and reverse)	Amplicon Length
		Test Genes			
Na/K-ATPase	*NKA*	Electrochemical gradient	*GQ153672.1*	CTGTCCTGAAAAGGGAATGCA TTTCCAATAGAAAGCTCAACACATTT	76
Na/HCO_3 cotransporter	*NBC*	Secondary active ion transport	*bankit1347543*	GGAAGAATGCATGAAAGACACAAT TCGCTTCATGTGTTGATGGAA	70
Na-driven Cl/HCO_3 exchanger	*NDCBE*	Secondary active ion transport	*bankit1347548*	AGGAGCTGAATCCGCCAAT AGCCGGTAGCTTGGTGGTT	65
Carbonic anhydrase	*CA*	Bicarbonate formation	*bankit1347557*	ACCTTTAGCCATCCGCTGAA TCCGTTGTTGGTGACTTCCA	66
ATP-synthase	*ATP-Synth*	Electron transport chain	*bankit1347571*	GGAGAGAGCTGCCAAGATGAA CCTGGGTCTCGATGACTGGTA	74
Cytochrome *P*-450	*CYP 450*	Xenobiotic defence	*bankit1347604*	CCGGCGGTGCCAGTTA TGCGGGAATTTTGTAATCATCA	69
Cytochrome-c- oxydase	*COX*	Electron transport chain	*YP514795*	TCCTCCTCCGCAGTTGAAAG GCCCGCATGTGATAAGTTACTAGA	81
Octopine dehydrogenase	*ODH*	Anaerobic metabolism	*AY545135*	GCCGAGTCAACCCGGTTT CGCTGGTTCGACCTCCAA	65
		Reference Genes			
Cleavage and polyadenylation specificity factor	*CPSF*	mRNA polyadenylation	*bankit1345716*	CACACCAGCCCATGAAAAGA GGTGGTGTTGGCGAGTATGC	68
Ubiquitin-conjugated enzyme	*UBC*	Protein degradation	*bankit1345727*	CAATAATACCGTGAAAGTGGCAGAT TTTCCTGAGCTTCATATATTTCATCAG	74

In Situ Hybridization

Isolated plasmids from the generated clones were used for the synthesis of antisense and sense RNA probes. Following PCR with T7 and SP6 primers, the products were subjected to in vitro transcription with T7 or SP6 RNA polymerase (Roche, Penzberg, Germany) in the presence of digoxigenin (dig)-UTP. Dig-labeled RNA probes were examined with RNA gels and dot-blot assays to confirm quality and concentration. For dot-blot assays, synthesized probes and standard RNA probes were spotted on nitrocellulose membrane according to the manufacturer's instructions. After cross-linking and blocking, the membrane was incubated with an alkaline phosphatase-conjugated anti-dig antibody and stained with nitro blue tetrazolium (NBT) and 5-bromo-4-chloro-3-indolyl phosphate. Fixed samples were immersed in PBS containing 30% sucrose overnight and then embedded in tissue-freezing medium (Jung Leica, Nussloch, Germany) at −20°C. Then 10-μm thick cryosections were generated with a cryotome (Leica, Heidelberg, Germany) and were transferred onto poly-L-lysine-coated slides. After washing with PBS-Tween (PBST; 0.1% Tween in PBS), slides were incubated with hybridization buffer (HyB) containing 60% formamide, 5× SSC buffer, and 0.1% Tween-20 in H_2O for 5 min at 70°C. Prehybridization was performed in HyB^+, which is the HyB supplemented with 200 μg/ml yeast tRNA and 100 μg/ml heparin for 2 h at 57°C. Following prehybridization, samples were incubated with the RNA probe diluted 1:2,000 in HyB^+ at 57°C overnight for hybridization. Samples were then washed at 65°C for 10 min in 100% HyB, 75% HyB, and 25% 2× SSC, 10 min in 50% HyB and 50% 2× SSC, 10 min in 25% HyB and 75% 2× SSC, and twice for 30 min in 2× SSC and incubated at 65°C. Samples were washed twice for 10 min in PBST at room temperature. After serial washings, slides were incubated for 1 h in preblocking solution containing 1% BSA and 20% sheep serum diluted in PBST for 2 h. Samples were then incubated in 1:2,000 alkaline phosphatase-conjugated anti-dig antibody in blocking solution overnight. Finally, samples were washed with PBST, and staining reactions were conducted with nitro blue tetrazolium and 5-bromo-4-chloro-3-indolyl phosphate in staining buffer (1 M Tris, pH 9.5; 1 M $MgCl_2$, 5 M NaCl; 0.1% Tween 20) (1:100) at 37°C until the signal was sufficiently strong. The staining reaction was terminated by several (2–3) washings with methanol, and slides were stored in PBS for further immunohistochemical stainings.

For immunocytochemical staining, mRNA probe hybridized slides were washed in PBS (pH 7.3) and exposed to a heat shock inside the PBS bath using a microwave (600 watts for 2 × 3 min). Afterward, samples were transferred to a PBS bath containing 150 mM NaCl and Tween 20 (concentration, 0.2 μl/ml) for 10 min, and a PBS bath containing 5% skimmed milk for 20 min to block nonspecific bindings. The primary antibody, a rabbit polyclonal antibody raised against an internal region of NKA-α_1 of human origin [Na^+/K^+ ATPase-α (H-300), Santa Cruz Biotechnology] was diluted in PBS to 10 μg/ml, placed in small droplets of 100 μl on the sections, and incubated for 2 h at room temperature in a wet chamber. To remove unbound antibody, the sections were then washed (3× 5 min) in PBS and incubated for 1 h with small droplets (100 μl) of secondary antibody, FITC-labeled goat anti-rabbit IgG (Santa Cruz Biotechnology). After rinsing in PBS (3× 5 min), sections were covered with a mounting medium and examined with a fluorescence microscope (Axio SCOPE A1; Zeiss, Hamburg, Germany) with an appropriate filter set (488-nm band-pass excitation filter). Brightfield and fluorescence images were acquired from in situ hybridized and immunohistochemically stained sections and merged using Adobe Photoshop CS2.

Statistical Analysis

Values are presented as means ± SE and compared using Student's *t*-test or one-way ANOVA followed by Tukey's post hoc tests using Sigma Stat 10.0 (Systat Software). Statistical analysis of qRT-PCR results was performed on mRNA quantities normalized to the geometric mean of the housekeeping genes *CPSF* and *UBC*.

RESULTS

Growth and PVF Abiotic Conditions

At the time point of PVF and gill sampling for qRT-PCR, all *S. officinalis* eggs contained viable embryos [stage 30, (59)] with fresh masses (FM) of 169.4 mg ± 8.8 mg (control, n = 15) and 161.9 ± 4.8 mg (0.37 kPa, n = 15) (Fig. 1*A*). All animals appeared fully differentiated, and organogenesis was complete. The DML of *S. officinalis* late-stage embryos was significantly different between control (6.91 ± 0.19 mm) and 0.37 kPa CO_2-treated animals (6.33 ± 0.17 mm). Hatchlings (2 days posthatch) were characterized by a significantly reduced body mass of 13% and a reduced DML by 40% in response to 0.37 kPa (Fig. 1*B*). Intermediate hypercapnia (0.16 kPa) did not cause growth delays in embryos and hatchlings. Juvenile growth rates were not significantly influenced during exposure to 0.37 kPa CO_2. Juvenile cuttlefish had an initial mass of 11.90 ± 2 g, and grew at rate of 0.13 ± 0.02 g/day under control and 0.20 ± 0.05 g/day under high CO_2 conditions, increasing body mass by ~50% during the 42-day trial.

The PVF was characterized by average pH values of 7.4 and a mean P_{CO_2} of 0.26 kPa under control conditions (Fig. 2, *A* and *B*). Under hypercapnia, PVF pH significantly decreased to 7.2 (seawater P_{CO_2}: 0.16 kPa) and 7.0 (seawater P_{CO_2}: 0.37 kPa). Hypercapnia led to additive increases in PVF P_{CO_2}. This resulted in a PVF P_{CO_2} of 0.45 kPa and of 0.78 kPa when exposed to seawater P_{CO_2} of 0.16 kPa and 0.37 kPa, respectively. Thus, CO_2 diffusion gradients were maintained even under relatively high seawater P_{CO_2}, suggesting maintained rates of metabolic CO_2 excretion.

qRT-PCR

In late-stage embryos and hatchlings, reduced somatic growth is accompanied with changes in mRNA expression of several genes. In gill tissues of late-stage embryos (Fig. 3*A*) significant 0.8 to 2.1 log2-fold (40 to 75%) downregulation was observed in response to 0.37 kPa CO_2 for the transcripts of ion-transporting proteins NKA, NBCe, and cCAII. *soNDCBE* showed no CO_2-dependent change in expression. At the intermediate P_{CO_2} of 0.16 kPa only two significant changes were observed in embryos: *NBCe* was 1.2 log2-fold downregulated and c*CAII* was upregulated (0.5 log2-fold). In hatchlings (Fig. 3*B*), a similar general expression pattern was observed with strong downregulation (up to 3.0 log2-fold; 85%) of all acid-base regulatory candidate genes (e.g., *NKA*, *NBCe* and c*CAII*) in response to 0.37 kPa CO_2. In addition, ATP-synthase, cytochrome-*c* oxidase subunit 1 (*COX*) and cytochrome *P*-450 (*CYP-450*) were significantly downregulated in hatchlings. At the intermediate P_{CO_2} of 0.16 kPa only two significant changes were observed: *1*) *NBCe* was 0.6 log2-fold downregulated, and *2*) *COX* was 0.3 log2-fold upregulated.

In juveniles, mRNA expression of all genes tested did not significantly differ between treatments after 2, 11, and 42 days of hypercapnia (Figs. 3*C* and 4). Although no differences between CO_2 treatments were measured, a significant increase in expression has been observed with time for several genes. For example *soNKA* was 0.11 log2-fold (+12.93%), *soNBCe* 0.23 log2-fold (+29.53%), *socCAII* 0.25 log2-fold (+33.64%) and *ODH* was 0.2 log2-fold (+25.39%) upregulated (Fig. 4). All genes related to ion transport showed a significant increase in expression over the course of the experimental period.

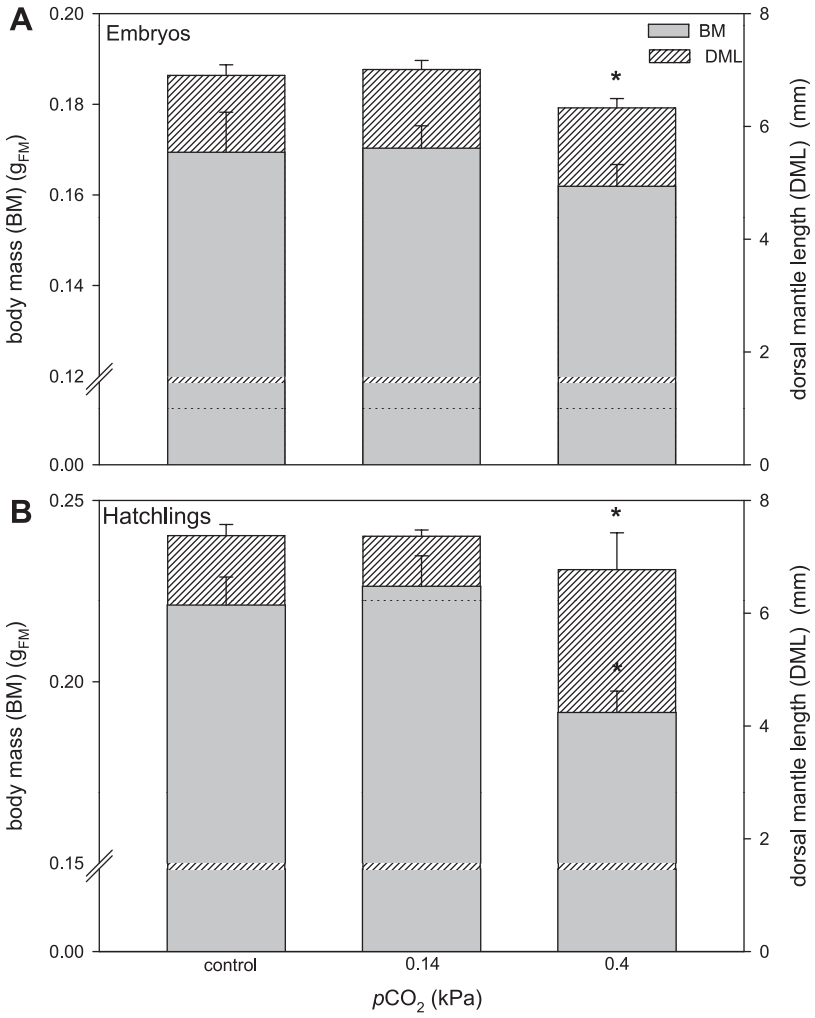

Fig. 1. Biometric information of embryos (*A*) and hatchlings (*B*) of *Sepia officinalis* reared under different CO_2 concentrations. The somatic growth is documented by the dorsal mantle length (DML) and their body mass (BM). *Significant differences between CO_2-treated and control animals. Bars represent mean ± SE (n = 15).

Gill NKA Activity and Protein

NKA maximum activities in gill tissues of juvenile cuttlefish steadily declined over the time course of the hypercapnia trial in the control and the CO_2 treatment (Fig. 5*A*). NKA maximum activity differed significantly between treatments after 48-h incubation with 94.8 ± 18.5 $\mu mol_{ATP} \cdot g_{FM}^{-1} \cdot h^{-1}$ at control P_{CO_2} and 112.5 ± 13.7 $\mu mol_{ATP} \cdot g_{FM}^{-1} \cdot h^{-1}$ at a seawater P_{CO_2} 0.3 kPa. From 48 h to 11 days, maximum activity was significantly increased by ~15% in CO_2-treated animals. At 42 days of incubation, no significant difference between control and CO_2-treated animals was observed.

NKA protein concentrations were determined by immunoblotting (Fig. 5*B*). Besides the strong immunoreactivity of a 100-kDa protein, further weaker bands were visible, which may be explained by unspecific binding of the polyclonal antibody used (see Supplemental Fig. S1). NKA protein tended to follow the patterns of the activity measurements at least for the time points of 48 h and 11 days, with increases of 16% and 34%, respectively. Similar, significantly higher protein levels were found after 11 days, whereas long-term acclimated hypercapnic juveniles displayed the same NKA protein content as the controls. After 42 days, NKA protein concentrations increased by 30–40%, matching the increased *NKA* mRNA expression by 20–25% at this time point. However, no transcriptional response was detected for *soNKA*, during both short- and long-term exposure to elevated seawater P_{CO_2} (Fig. 5*C*).

Localization of Ion Transporters in Gill Tissues

To identify the cell types that specifically express *soNKA*, *soNBCe* and *soV-AH* mRNA, in vitro synthesized RNA probes were used to detect mRNA of these proteins in cryosections of gills of *S. officinalis* juveniles. Subsequent immunocytochemical labeling with an anti-NKA α-subunit antibody was carried out (Figs. 6 and 7*B*).

In gill tissues of *S. officinalis* the *NKA* mRNA was predominantly expressed in the concave part (3rd-order lamellae) of the transport active epithelium of the entire second-order lamellae (Figs. 6*A* and 7*A*). The cells of this transport active epithelium are higher and more voluminous compared with those of the outer respiratory epithelium (Fig. 6*A*). Furthermore, the localization of NKA by immunocytochemistry demonstrates *NKA* transcript and protein to be colocalized in ionocytes of the inner epithelium (Fig. 6*A*). The concentration of the enzyme was high in basolateral regions (close to the blood sinus) (Fig. 6). Furthermore, *soNBCe* (Fig. 6*B*) and *soV-HA* (Fig. 6*C*) transcripts were also detected in cells of the inner transport active epithelium of third-order gill lamellae. Merged images of NKA immunocy-

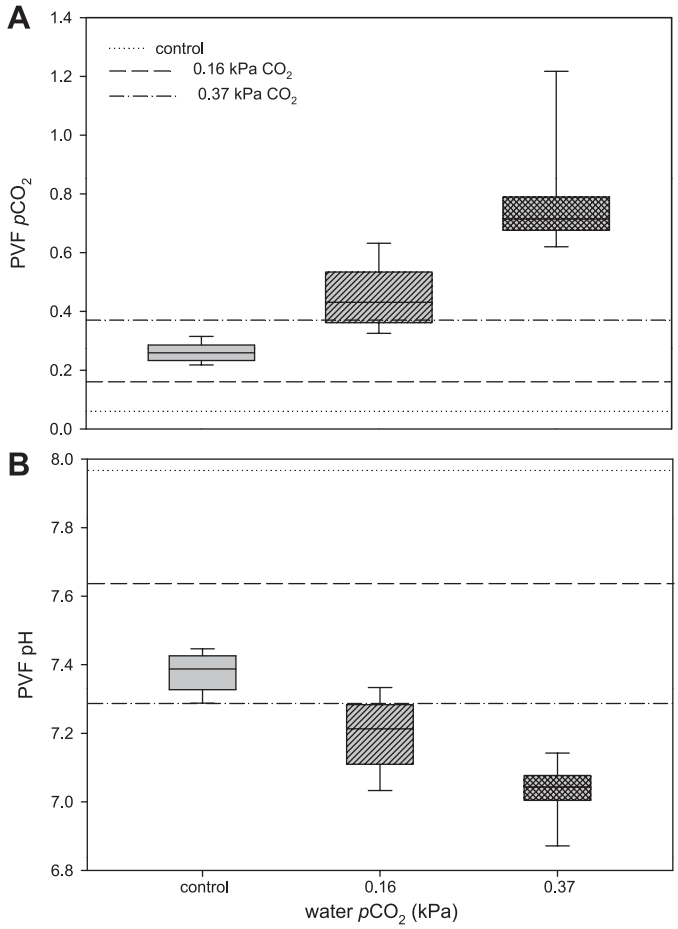

Fig. 2. Abiotic parameters determined in perivitelline fluid (PVF) of *S. officinalis* and in the experimental sea water. *A*: PVF CO_2 concentrations were calculated from pH and dissolved inorganic carbon (C_T) at different ambient P_{CO_2}. *B*: pH of the PVF at different ambient P_{CO_2}. Dotted and dashed lines inserted into the graph represent the ambient water pH and P_{CO_2}, respectively. Values are given as means including 5th (bars) and 95th (boxes) percentiles (n = 15). Boxes: control, gray; 0.16 kPa CO_2, slashed; 0.37 kPa CO_2, hatched.

tochemistry and in situ hybridization demonstrate that NKA protein and mRNA, *soNBCe* mRNA, and *soV-HA* mRNA are colocalized in ion transporting cells of the inner epithelium of the third-order gill lamellae.

DISCUSSION

Effects of moderate hypercapnic stress on marine organisms recently moved into the focus of research due to rising atmospheric CO_2 levels in the atmosphere, which lead to an acidification of the oceans (24, 64, 73). The present study investigated responses to environmental hypercapnia in different life stages of the cephalopod *S. officinalis*. On the organismic level, we observed reduced somatic growth under 0.37 kPa CO_2 in early developmental stages. On the protein level, the characterization of NKA in juveniles revealed an increased activity and protein concentration under elevated seawater P_{CO_2} (~0.3 kPa) during short-term incubation. To address the response of the acid-base regulating machinery, we cloned genes that may play a key role in pHe compensation under hypercapnic conditions, such as *soNKA*, *soNBCe*, *soNDCBE*, *socCAII*, and *soV-HA*. Dynamic changes in gene expression could be observed in late-stage embryos and hatchlings, but no CO_2-related expression responses were observed in juveniles during short- and long-term incubation. Finally, immunohistology and in situ hybridization showed for the first time that gills of cephalopods exhibit specialized cells in the inner, transport-active epithelium that express *soNKA*, *soNBCe*, and *soV-HA*.

Growth and PVF Abiotic Conditions

As adult fish (29, 31), juvenile cephalopods can tolerate high seawater P_{CO_2} of up to 0.6 kPa over long exposure

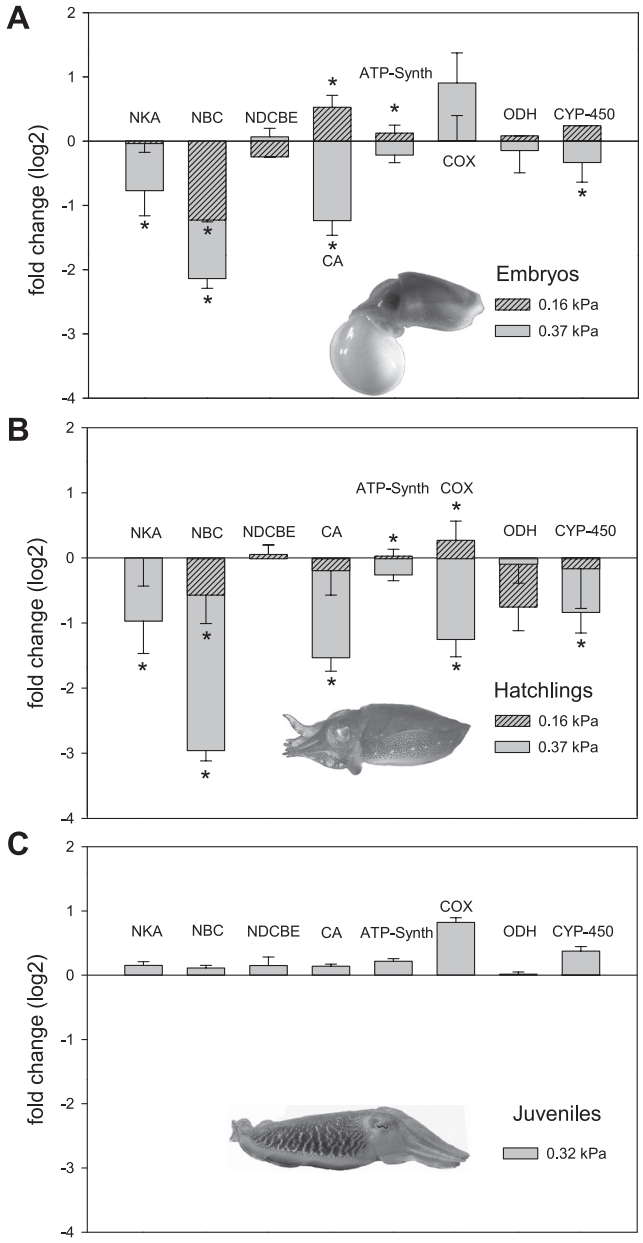

Fig. 3. Expression profiles from selected genes determined for gill tissues of different ontogenetic stages of *S. officinalis*. Embryos (*A*) and hatchlings (*B*) were incubated at 3 different P_{CO_2} values (control, 0.16, and 0.37 kPa) for 4 wk until hatching, whereas juveniles (*C*) were incubated for 6 wk at a P_{CO_2} of 0.32 kPa. Expression of the gene candidates are normalized to the geometric mean of *soCPSF* and *soUBC*. *Significant change in gene expression (n = 8–10).

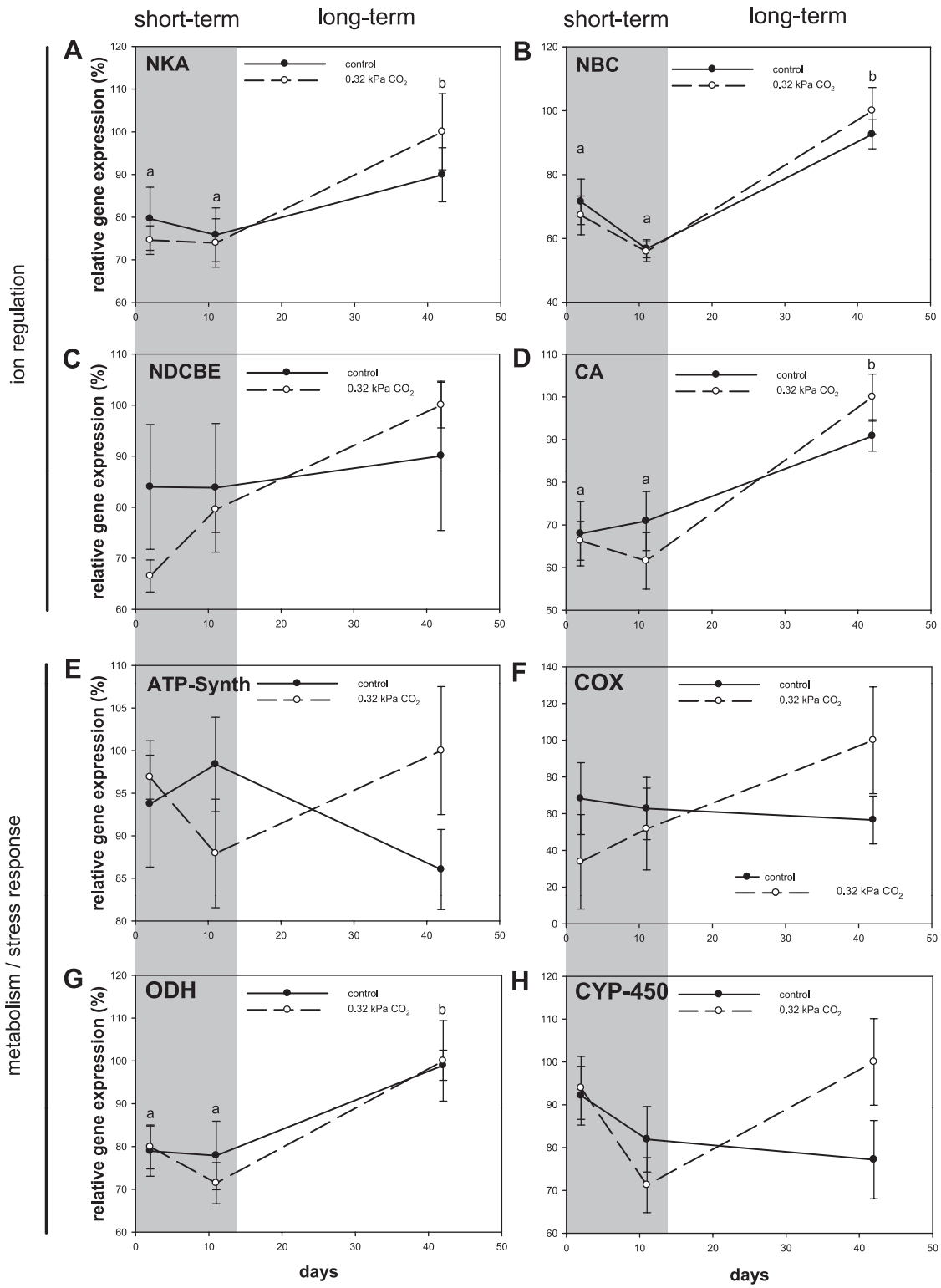

Fig. 4. Juvenile *S. officinalis* gill mRNA expression of gene candidates related to ion regulation (*A–D*), metabolism (*E–G*), and stress (*H*) during 48 h, 11 days, and 42 days of exposure to 0.3 kPa hypercapnia. Expression of the gene candidates are normalized to the geometric mean of *soCPSF* and *soUBC* and given in % of the maximum expression of each gene tested. No significant differences were observed for the expression of genes between treatments. [a,b]Letters denote a significant difference between each time point and values are expressed as means ± SE ($n = 8$).

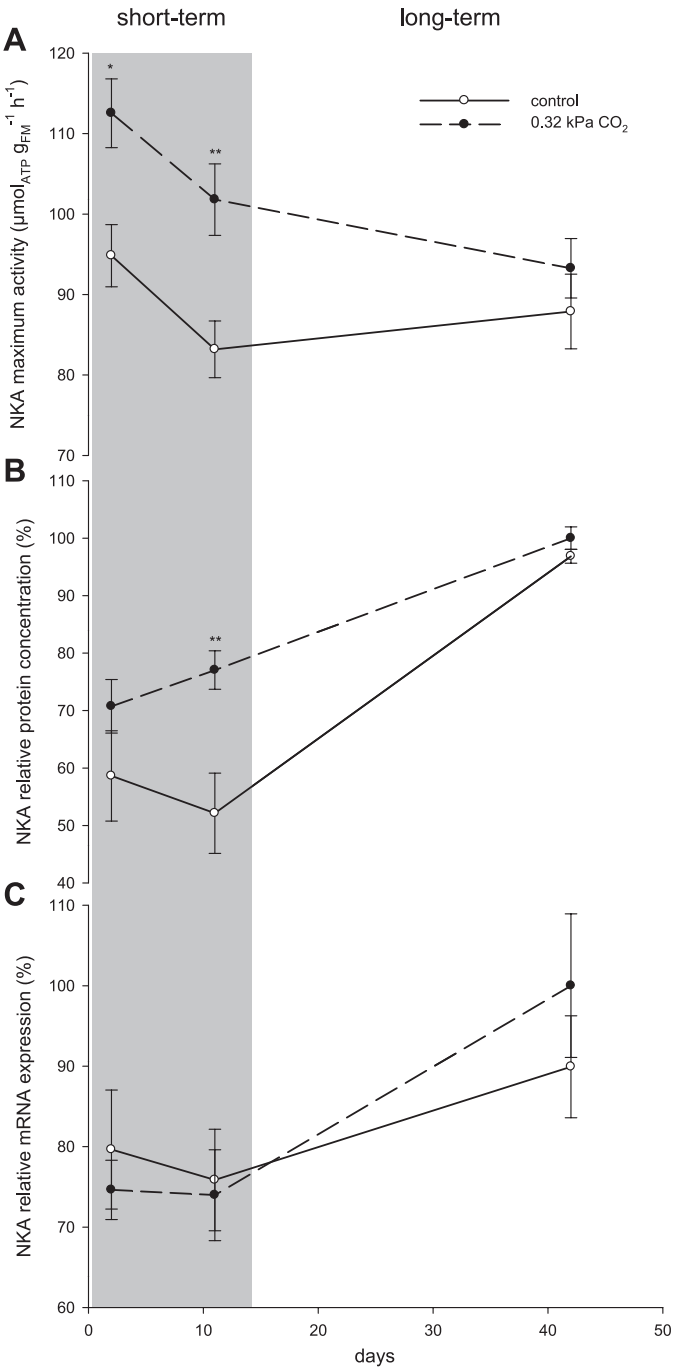

Fig. 5. Juvenile *S. officinalis* specific gill Na^+/K^+-ATPase (NKA) maximum activity (*A*), relative protein concentration (*B*) and relative mRNA expression (*C*) in control (0.04 kPa) and CO_2-treated (0.3 kPa) animals at the 3 time points 48 h, 11 days, and 42 days. Activity is given (in µmoles $ATP \cdot g_{FM}^{-1} \cdot h^{-1}$, where FM is fresh mass). Expression Na^+/K^+-ATPase is normalized to the geometric mean of *soCPSF* and *soUBC* and given in % of the maximum expression determined. Significant differences compared with the control group (*$P < 0.05$; **$P < 0.01$; Student's *t*-test). Values are means ± SE ($n = 6–8$).

times without suffering from decreased growth and calcification (43). However, the present study demonstrates that even if juveniles or adults tolerate high P_{CO_2}, early life stages are more susceptible toward environmental hypercapnia. Hypercapnia- induced reductions in larval and embryonic growth have also been observed in several other invertebrate species such as copepods, echinoderms, and bivalves (20–22, 54–56).

The increased sensitivity of cephalopod early life stages could be due to two primary reasons. The first is related to gill development; similar to the situation in fish and decapod crustaceans, the cephalopod gill is the most important site for ion regulatory processes (49, 75). During larval development, rudimentary gill structures occur at stage 20 and significantly differentiate over the course of embryonic development as well as after hatching (1, 75). Schipp et al. (75) demonstrated that the cephalopod gill changes morphogenetically within several days after hatching to become a highly folded epithelium with a high density of vesicles, mitochondria, and a high concentration of cCA and NKA. This differentiation indicates that gas exchange and ion regulatory capacity might be fully activated only after leaving the protective egg capsule. This could partially explain the higher susceptibility of embryonic stages to environmental hypercapnia.

Furthermore, the abiotic conditions in the PVF are directly influenced by the P_{CO_2} of the surrounding seawater (Fig. 2). Cephalopod embryos are exposed to very low P_{O_2} values (<6 kPa, ~28% air saturation) during the final phase of embryonic development. This is due to increasing metabolic rates and the egg casing acting as a diffusion barrier for dissolved gases (14). On the flip side, this diffusion limitation not only decreases P_{O_2} inside the egg, but also results in PVF P_{CO_2} values > 0.3 kPa and pH values < 7.5 under control conditions (40). The present results indicate that environmental P_{CO_2} is additive to the natural accumulation of CO_2 in the PVF, leading to very high PVF P_{CO_2} of up to 0.5 and 0.7 kPa inside the egg at a seawater P_{CO_2} of 0.16 or 0.37 kPa, respectively. This almost linear increase of PVF P_{CO_2} is necessary to conserve the CO_2 diffusion gradient across the egg capsule that drives excretion of metabolic CO_2 to the seawater. Thus, alterations in environmental P_{CO_2} create a greater challenge to the developing embryo compared with juveniles or adults. This is particularly striking, as cephalopod blood P_{CO_2} typically is 0.2–0.3 kPa higher than that of the surrounding medium (41, 72). It is therefore reasonable to expect a blood P_{CO_2} in the 0.7–1.0 kPa range in the hypercapnic embryos of this study. These conditions may lead to metabolic depression, which has been suggested to be elicited by extracellular acidosis in some marine invertebrates including the sipunculid worm *Sipunculus nudus* (73). However, adult cuttlefish have been shown to be able to accumulate millimolar concentrations of HCO_3^- in their blood in response to hypercapnia to stabilize pHe [see below (41)]. If embryonic *S. officinalis* also respond with a similar pHe compensatory reaction with respect to the high extracellular P_{CO_2} encountered during hypercapnia, this may represent a severe energetic challenge and could result in a higher fraction of aerobic scope spent on acid-base regulation. Both, a (potential) hypercapnia-induced metabolic depression and increased energy allocation toward ion regulatory processes would most likely have negative repercussions on embryonic growth. Future studies need to determine the extracellular acid-base regulatory capacity of embryonic cephalopods.

Gene Expression

Gene expression profiles revealed strong differences between early developmental stages (late embryos and hatch-

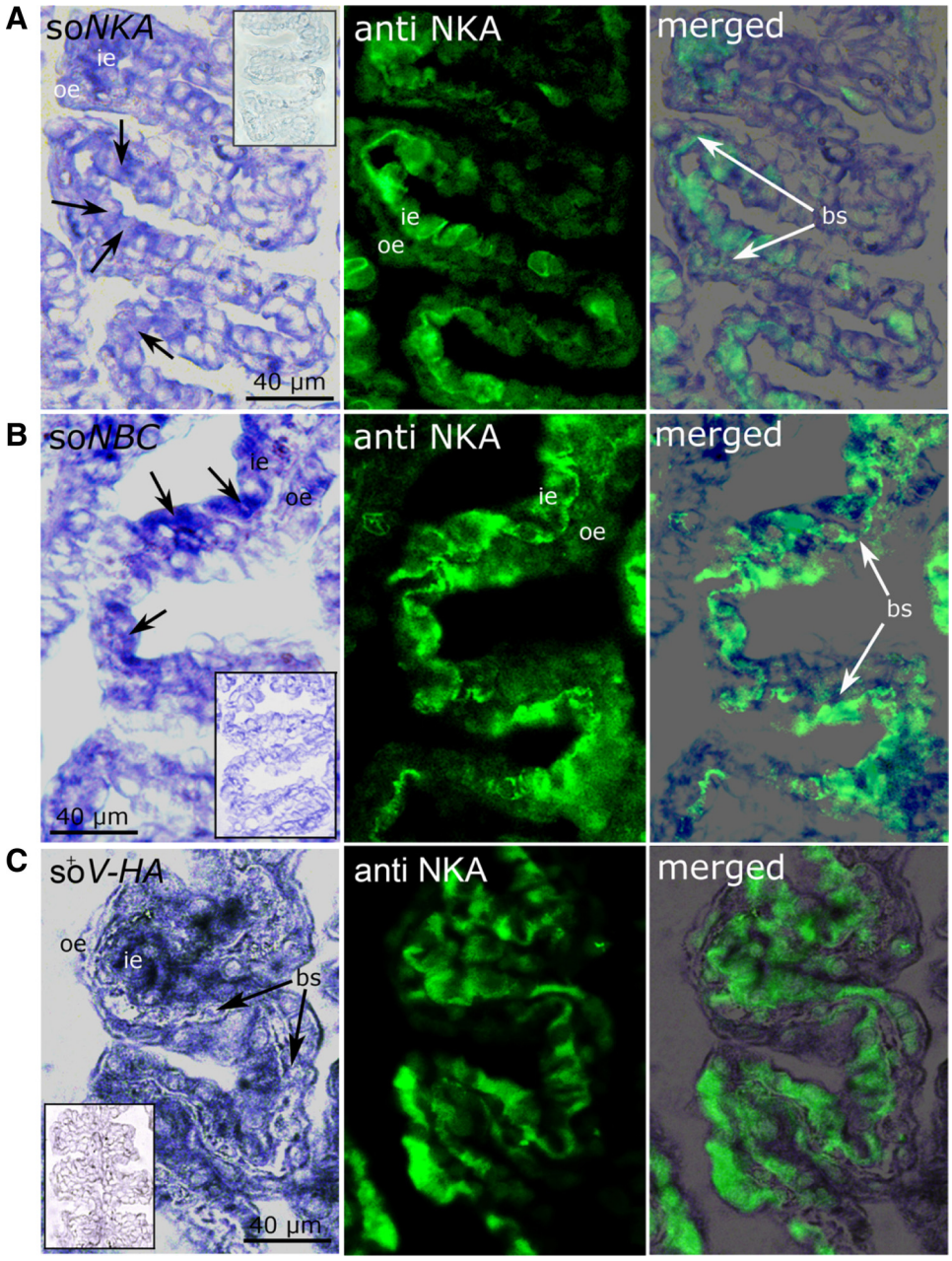

Fig. 6. Expression of *soNKA*, *soNBC*, and *soV-HA* in cells of the inner epithelium (ie) of the 3rd-order gill lamellae of juvenile *S. officinalis*, reared under control conditions, visualized by in situ hybridization. *A*: large cells in the inner (ie) transport active epithelium of the gill lamellae are rich in *NKA* (arrows), while the outer (oe) is thin and exclusively involved in respiratory processes. *B*: merged image demonstrates that NKA protein and *soNBC* mRNA are colocalized in ion transporting cells of the inner epithelium. *C*: furthermore, *soV-HA* is coexpressed in NKA-rich cells of the transport active epithelium. The oe and the ie are lining a blood sinus (bs). *Inserts*, *left*: hybridization with a sense mRNA probe as the negative control.

lings) compared with 6-mo-old juveniles. In late embryos and hatchlings exposed to 0.37 kPa CO_2 for 5 wk, reduced somatic growth is accompanied by changes in the expression of several genes that are involved in ion regulatory (e.g., *soNKA*, *soNBCe*, *socCAII*) and metabolic (e.g., *ATP-synthase*, *COX*, *CYP450*) processes. Intriguingly, mRNA of all acid-base regulation gene candidates (*soNKA*, *soNBCe*, and *socCAII*), were downregulated by up to 80% in response to elevated seawater P_{CO_2}.

The significant downregulation of the gene candidates is also likely causally linked to a developmental delay in the embryos. Large differences in mRNA expression profiles have been attributed to a hypercapnia-induced developmental delay in sea urchin larvae (e.g., M. Stumpp, S. Dupont, M. C. Thorndyke, F. Melzner, unpublished observation). Thus, strong differences in mRNA expression could be indirect hypercapnia effects. For example, in larvae of *Strongylocentrotus purpuratus NKA*, mRNA levels peak during gastrulation (25 h postfertilization) followed by an ~100% decline to trace levels at 60 h postfertilization (61). Thus, a slight difference in developmental rate would cause large changes in *NKA* mRNA expression. Delays in developmental rate of early life stages in response to hypercapnia have been found in several marine invertebrate species (21, 22). Interestingly, when *S. officinalis* late-stage embryos were exposed to 0.16 kPa CO_2 only *socCAII* exhibited an increased expression. Accordingly, an upregulation of *socCAII* in gills of late-stage *S. officinalis* embryos subjected to seawater P_{CO_2} of 0.16 kPa (0.45 kPa PVF P_{CO_2}) would support a role of this enzyme in active pHe regulation. However, while no significantly reduced somatic growth was observed in 0.16 kPa embryos and hatchlings, a significant downregulation of ion regulatory genes, especially *soNBC*, was detected. A pos-

sible explanation for this phenomenon could be a slight delay in gill differentiation and, thus, expression of ion regulatory genes despite similar body dimensions. It is important to note that during the transition phase from embryo to hatchling, the cephalopod gill is subject to strong proliferation (49, 75). More detailed histological studies are needed to resolve whether altered expression profiles under moderate hypercapnic stress are related to varying degrees of gill epithelia differentiation. The consistent strong downregulation of acid-base relevant genes (e.g., *soNKA*, *soNBC*, and *socCAII*) in response to 0.37 kPa water P_{CO_2} (0.75 kPa PVF P_{CO_2}), suggests that the former transporters might be coregulated as a functional unit. The location and function of acid-base relevant transporters are discussed in greater detail below.

The expression patterns of ATP-synthase, which is the key enzyme in ATP synthesis, correlates with those of the ion regulatory genes, which suggests a coupling of metabolic (e.g., energy providing) and ion regulatory (energy consuming) processes. This observation is supported by a significant hypercapnia-induced downregulation of *COX* mRNA levels, at least in hatchlings. In addition, CYP-450, which is involved in the metabolism/oxidation of endogenous organic compounds such as lipids, steroidal hormones, and exogenous xenobiotics (e.g., 65), was significantly downregulated in embryos and hatchlings. This indicates that the development of ion regulatory epithelia is tightly coupled to metabolic capacities. It has been previously shown that the proliferation of gill epithelia involves mitochondrial proliferation as well (75).

In juveniles, no significant hypercapnia-dependent responses in gene expression were found during the course of the experiment, which indicates that routine expression profiles are sufficient for the organism to cope with elevated P_{CO_2} up to 0.3 kPa. A CO_2-independent increase in mRNA expression along the experimental interval has been observed for all ion regulatory genes (except *soNDCBE*) studied (Fig. 4), which again supports the hypothesis that acid-base regulatory gene candidates in gill tissues are coregulated. The observed increase in expression during the 42-day interval is probably closely related to growth and feeding rate, as the animals increased their body mass by ~50% during the experiment at a rate of 1.43% per day. Body mass, feeding, and growth rates are directly related to differences in specific metabolic rate, enzyme activities, and mRNA expression (33, 38, 66, 78, 88).

Effects of Hypercapnia on NKA

In juvenile *S. officinalis*, two distinct hypercapnia acclimation phases were observed with respect to *soNKA* mRNA expression, protein concentration, and maximum activity. The first phase is a short-term response (<11 days), and the second is a long-term acclimation phase (42 days). After 11 days, NKA maximum activity was 15% higher under hypercapnia compared with control conditions, which was also reflected in a higher NKA protein concentration. This increase indicates a higher energetic demand to maintain the electrochemical gradient across the cell membrane and thus higher acid-base regulatory capacities in response to elevated water P_{CO_2}. These findings correspond to the strong pHe compensation reaction that was observed in the same species; *S. officinalis* elevates blood HCO_3^- from 3.4 to 10.1 mmol [HCO_3^-] in response to acute hypercapnia (0.6 kPa CO_2) (42). It is likely that the elevated gill NKA activity supports this pH regulatory response. Similar observations were made for Atlantic cod *G. morhua* and eelpout *Zoarces viviparus* exposed to 0.3 kPa and 1.0 kPa CO_2, respectively. NKA activities increased within the first days upon hypercapnic exposure in eelpout, and in both teleosts NKA activity almost doubled in response to long-term 0.6 kPa CO_2 exposure (15, 63). However, it cannot be excluded that besides gill epithelia, alternative sites (e.g., gut, kidneys) may also play a role in these compensatory processes. Long-term acclimation of 42 days revealed a decrease of NKA activity and protein concentration in *S. officinlis* gills back to control levels. One possible explanation for this effect could be the energetic favorable reorganization of physiological features to cope with this relatively moderate environmental stressor. In this respect, reversible phosphorylation of the α-subunit by several protein kinases (PKA, PKC, PKG, tyrosine kinase) was reported to modulate NKA activity in vertebrates and invertebrates such as gastropods (2, 10, 74). This posttranslational modulation of NKA activity may also explain the seemingly inconsistent results of NKA enzyme activity, protein concentration, and mRNA expression in response to acid-base disturbances (e.g., 26). Furthermore, the phospholipid composition of biological membranes can be directly linked to ion permeability and enzyme (e.g., NKA) activity in gills of fish and crustaceans and might be a key element that undergoes modification during hypercapnia acclimation (8, 53, 67, 82). Long-term maintenance of elevated NKA activity is an energetically expensive way to counter ionic disturbances (25, 33). The reduction of gill NKA activity after 42 days of hypercapnia suggests that long-term acclimation is probably accomplished without (a significant) rearrangement of the energy budget. This is crucial for maintenance of control rates of somatic growth and calcification, as observed in a growth trial with juvenile *S. officinalis* exposed to a P_{CO_2} of 0.6 kPa for 6 wk (43).

Acid-Base Regulation

Active organisms like fish and cephalopods exhibit a sophisticated ion regulatory machinery that is beneficial in coping with acid-base disturbances caused by respiratory acidosis, and might preadapt species to cope with future environmental hypercapnia through ocean acidification (11, 64, 77). The present work demonstrates for the first time that gene transcripts essential for acid-base regulation in teleost fish (50, 51, 83) are also found in the gill of the cephalopod mollusc *S. officinalis*. Earlier work by Schipp et al. (75) already demonstrated high concentrations of cCA in the transport active cells of the inner epithelium but only low concentrations in the outer, respiratory epithelium. Our findings demonstrate that NKA-rich cells in the cephalopod gill exhibit a set of enzymes that have been shown to be fundamental for pHe homeostasis in vertebrates.

For the two HCO_3^- transporters belonging to the SLC4 solute carrier family, sequence alignments show a maximum identity of 83% (*soNBCe*) and 100% (*soNDCBE*) compared with the respective sequences from the squid *Loligo pealei*. Electrophysiological studies demonstrated that base equivalent transport by squid *NBCe* is electrogenic with a 1:2 stochiometry, whereas *NDCBE* is electroneutral, achieving the exchange of one external Na^+ for one internal Cl^- and the inward flux of

two base equivalents (71, 85). The relative expression of these two HCO_3^- transporters in *S. officinalis* gill tissues revealed that *soNBCe* is expressed at least one order of magnitude higher than *soNDCBE* in cuttlefish gill. This finding corresponds to studies that cloned and characterized *NBCe* and *NDCBE* orthologues in the squid *Loligo pealei*, demonstrating their presence in giant fiber lobes, olfactory lobes, heart, and gills (71, 85). On one hand, Northern blot analysis revealed strong signals for *NDCBE* in olfactory and giant fiber lobes but only weak signals in gills and heart. On the other hand, a high expression of squid electrogenic *NBCe* was detected in gills and heart but not in olfactory and giant fiber lobes (71). Piermarini et al. (71) suggested that *NBCe* in gills of squid could be involved in HCO_3^- uptake similar to the situation in the vertebrate kidney. In the renal proximal tubule, HCO_3^- reabsorption is achieved via electrogenic NBCe1-A, which is located basolaterally. The basolateral HCO_3^- efflux is also accompanied by a decrease in intracellular [Na^+], which may also enhance proton excretion via NHE across both apical and basolateral membranes (3, 5). The majority of protons are excreted into the lumen of the tubule via different NHE isoforms located in the brush-border membrane of the proximal tubule (36, 87). Genetic knockout demonstrated that among these NHE isoforms, NHE-3 mediates up to 50% of the total NHE activity in this epithelium (87). Moreover, up to 40% of the proximal tubule HCO_3^- reabsorption is Na^+ independent and is sensitive to bafilomycin inhibition, which supports the involvement of V-type H^+-ATPase (86). Following acidification of the lumen, secreted H^+ and filtered HCO_3^- form H_2O and CO_2 catalyzed by extracellular membrane-bound carbonic anhydrase IV, and CO_2 diffuses into the tubule cells where it reacts with H_2O to form HCO_3^- mediated by cCAII. The generated HCO_3^- is reabsorbed into the blood via basolateral electrogenic Na^+/HCO_3^- cotransporters (3, 86).

We hypothesize that active HCO_3^- accumulation in body fluids, and thus pHe regulation in cephalopods, are potentially achieved according to the hypothetical model depicted in Fig. 7*C*. In this model HCO_3^- is formed via CO_2 hydration in the cytosol by cCAII. The central role of cytosolic CAII in regulating acid-base balance was studied in great detail for both fish and crustaceans (34, 35, 44–46, 70). For example, Georgalis et al. (32) provided direct evidence for a role of gill cCAII in regulating acid-base balance during exposure to 0.8 kPa CO_2 by demonstrating a 20% reduction in branchial acid efflux in trout subjected to CA inhibition. Subsequently, the increased intracellular [HCO_3^-] and negative membrane potential created by the sodium pump could drive electrogenic efflux of Na^+ and HCO_3^- across the basolateral membrane through NBCe. Acid secretion on the apical membrane could be achieved by V-type H^+- ATPase or a so far unidentified NHE-like protein.

Perspectives and Significance

The present work corresponds with earlier findings (41, 43) in demonstrating that juveniles of the cuttlefish *S. officinalis* can tolerate up to 6 wk exposure to elevated seawater P_{CO_2} (0.3

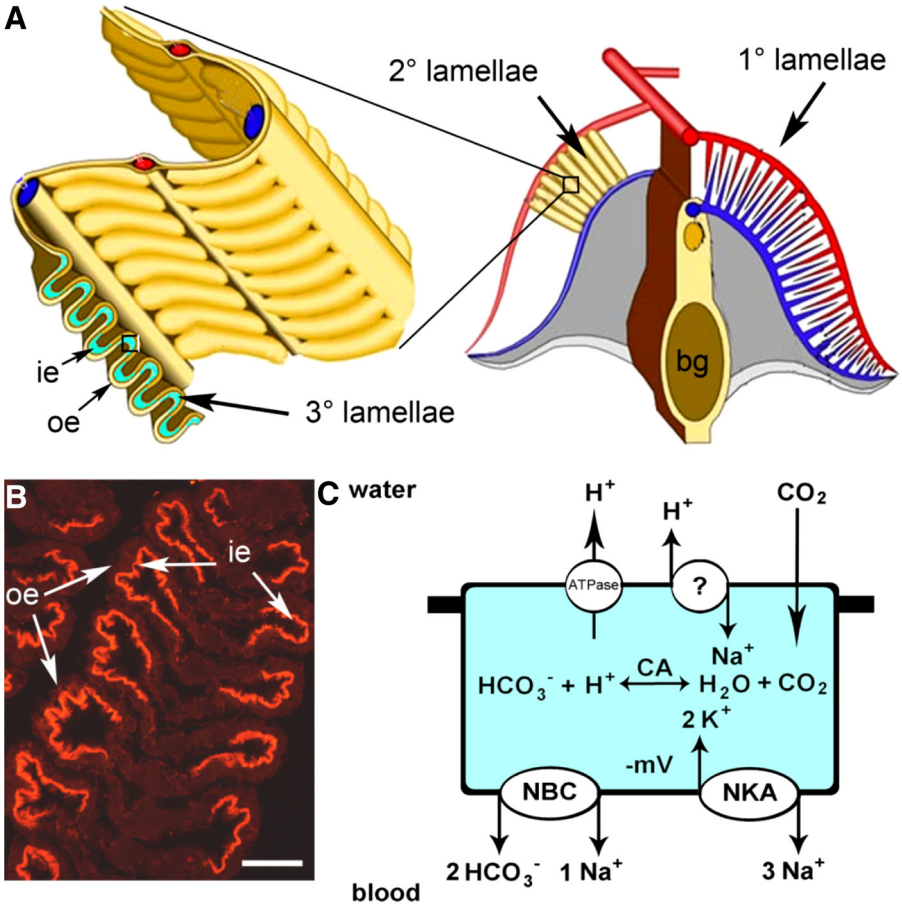

Fig. 7. *A*: diagram of the gill morphology of *S. officinalis*, indicating the arrangement of 1st-to-2nd-order lamella located on both lateral sides of the branchial gland (bg), showing the folded lamellae of the gill of *S. officinalis*. The concave ie of the 3rd-order gill lamellae belongs to the transport-active epithelium, whereas the oe is exclusively involved in respiratory processes. *B*: drawings adopted and modified from Young and Vecchione (89). Immunohistochemical staining of a gill lamellae, demonstrating NKA to be exclusively located in the ie of the 3rd-order lamellae. Scale bar = 50 μm. *C*: hypothetical model of a cell in the transport-active ie (rectangular sector in *A*) equipped with various transporters that are involved in acid-base regulatory processes. CO_2 is hydrated by carbonic anhydrase (CA) after diffusive entry resulting in HCO_3^- and H^+. Net accumulation of extracellular HCO_3^- is supported by the basolateral NBC. Net proton extrusion is possibly achieved by apical NHE-like protein powered by elevated Na^+/K^+-ATPase activity in the basolateral membrane.

kPa CO_2) without significantly altering mRNA expression profiles of potential key acid-base regulatory and metabolic enzymes. Although transient and moderate responses were found on the NKA protein level, routine expression of genes coding for important ion regulatory proteins seem to be sufficient to cope with a CO_2-induced acidosis up to 0.3 kPa CO_2. Transcripts of key enzymes of metabolism, such as ATP-synthase, cytochrome-*c* oxidase and octopine dehydrogenase did not respond to hypercapnia stress, indicating the possibility that energy demand is not greatly increased by the severity of abiotic stress applied. These observations support the hypothesis that active organisms like adult teleost fish and cephalopods can tolerate long-term exposure to elevated water P_{CO_2} comparatively well. The ability of such active ectothermic organisms to tolerate environmental hypercapnia is most likely linked to their high ion regulatory capacity. Nevertheless, several studies have demonstrated that a hypercapnia-induced acid-base disturbance that is compensated via HCO_3^- accumulation in body fluids may lead to a hypercalcification of $CaCO_3$ structures, such as fish otoliths, crustacean carapaces, and cephalopod cuttlebones (9, 42). In the long run, hypercalcification of structures responsible for buoyancy and balance control may negatively influence swimming behavior, active metabolism, and prey capture.

This study also demonstrated that embryos may respond more sensitively to environmental stress than adults, indicated by a reduced hatching size and delayed development. It can be hypothesized that the degree of sensitivity is related to the presence and capacity of ion regulatory structures. The ontogeny of ion regulatory epithelia (e.g., gills) were demonstrated to differ significantly within the group of coleoid cephalopods, suggesting a higher vulnerability in those with a planktonic type of larval development (49). It has been hypothesized that smaller cephalopod hatchlings would need more time to escape from the "window of vulnerability" (69), and thus, elevated P_{CO_2} may negatively influence their survival due to increased predation. As a consequence, even if elevated CO_2 levels are tolerable for juveniles or adults, cephalopod populations may still be affected due to the decreased fitness and survival of embryos and hatchlings.

The higher sensitivity in early life stages is most probably due to the fact that increases in environmental P_{CO_2} are additive to the naturally high P_{CO_2} (up to 0.4 kPa) of the PVF. This leads to extreme hypercapnic conditions (P_{CO_2} up to 0.7 kPa) inside the egg. Furthermore, an increased sensitivity may also be explained by the incomplete development and functionality of ion regulatory epithelia in early developmental stages (28, 75). The characterization of these gill epithelia provided evidence that specialized cells contain a set of specific enzymes that are most likely involved in controlling pHe homeostasis. The cephalopod gill acid-base regulatory machinery, consisting of NKA-rich cells, equipped with proteins such as NBCe, cCAII, and V-HA, shows a convergent evolution pattern to that of decapod crustaceans and teleost fish. Expression pattern of acid-base regulatory genes in early cephalopod life stages responded in an opposed manner as described for marine fish and crustaceans most likely due to a developmental delay and thus not due to direct action of elevated P_{CO_2}. However, the present study provides a first mechanistic platform for future research on ion regulation in a powerful acid-base regulating marine invertebrate. The application of noninvasive electrophysiological methods such as ion-selective electrodes in combination with specific inhibitors will be crucial to gain deeper insights into the function of putative transporters in cephalopod gill epithelia. Future comparative studies should focus on the detailed characterization of key acid-base regulatory proteins in a variety of marine ectothermic animals to contribute toward a general understanding of the evolution and common principles of pHe regulation mechanisms.

ACKNOWLEDGMENTS

The authors thank T. Reusch for use of his qRT-PCR machine, and we are grateful to N. Bergmann and U. Panknin for valuable advice and help with carrying out the qRT-PCR assays.

GRANTS

This study was partly funded by a German (DFG) Excellence Cluster Future Ocean Grant (to F. Melzner) and a German Academic Exchange Service/National Science Council of Taiwan ROC, Project-Based Personal Exchange Programme Grant, project 50128946 (to F. Meizner and P. P. Hwang of the Institute of Cellular and Organismic Biology, Academia Sinica, Taiwan). This work is a contribution to the German Ministry of Education and Research funded project Biological Impacts of Ocean ACIDification subproject 3.1.3 (awarded to F. Melzner, M. A. Gutowska, and M. Lucassen).

DISCLOSURES

No conflicts of interest, financial or otherwise, are declared by the author(s).

REFERENCES

1. **Arnold JM.** Normal embryonic stages of the squid, *Loligo pealii* (Lesueur). *Biol Bull* 128: 24–32, 1965.
2. **Bertorello AM, Katz AI.** Regulation of Na^+-K^+-pump activity: pathways between receptors and effectors. *News Physiol Sci* 10: 253–259, 1995.
3. **Boron WF.** Acid-base transport by the renal proximal tubule. *J Am Soc Nephrol* 17: 2368–2382, 2006.
4. **Boron WF.** Regulation of intracellular pH. *Adv Physiol Educ* 28: 160–179, 2004.
5. **Boron WF, Boulpaep EL.** Intracellular pH regulation in the renal proximal tubule of the salamander: basolateral HCO_3^- transport. *J Gen Physiol* 81: 53–94, 1983.
6. **Caldeira K, Wickett ME.** Anthropogenic carbon and ocean pH. *Nature* 425: 365, 2003.
7. **Cameron JN, Iwama GK.** Compensation of progressive hypercapnia in channel catfish and blue crabs. *J Exp Biol* 133: 183–197, 1987.
8. **Chapelle S, Dandrifosse G, Zwingelstein G.** Metabolism of phospholipids of anterior or posterior gills of the crab *Eriocheir sinensis* during the adaptation of this animal to media of various salinities. *J Biochem* 7: 343–351, 1976.
9. **Checkley J, David M, Dickson AG, Takahashi M, Radich JA, Eisenkolb N, Asch R.** Elevated CO_2 enhances otolith growth in young fish. *Science* 324: 1683, 2009.
10. **Chibalin AV, Ogimoto G, Pedemonte CH, Pressley TA, Katz AI, Féraille E, Berggren PO, Bertorello AM.** Dopamine-induced endocytosis of Na^+/K^+-ATPase is initiated by phosphorylation of Ser-18 in the rat α-subunit and is responsible for the decreased activity in epithelial cells. *J Biol Chem* 274: 1920–1927, 1999.
11. **Choe KP, Evans DH.** Compensation for hypercapnia by a euryhaline elasmobranch: effect of salinity and roles of gills and kidneys in fresh water. *J Exp Zool A Comp Exp Biol* 297: 52–63, 2003.
12. **Claiborne JB, Evans DH.** Acid-base balance and ion transfers in the spiny dogfish (*Squalus acanthias*) during hypercapnia–a role for ammonia excretion. *J Exp Zool* 261: 9–17, 1992.
13. **Claiborne JB, Heisler N.** Acid-base regulation and ion transfers in the carp (*Cyprinus carpio*) during and after exposure to environmental hypercapnia. *J Exp Biol* 108: 25–43, 1984.
14. **Cronin ER, Seymour RS.** Respiration of the eggs of the giant cuttlefish *Sepia apama*. *Mar Biol* 136: 863–870, 2000.
15. **Deigweiher K, Koschnick N, Pörtner HO, Lucassen M.** Acclimation of ion regulatory capacities in gills of marine fish under environmental

hypercapnia. *Am J Physiol Regul Integr Comp Physiol* 295: R1660–R1670, 2008.
16. **Dickson A, Millero F.** A comparison of the equilibrium constants for the dissociation of carbonic acid in seawater media. *Deep Sea Res A* 34: 1733–1743, 1987.
17. **Dickson AG, Afghan JD, Anderson GC.** Reference materials for oceanic CO_2 analysis: a method for the certification of total alkalinity. *Mar Chem* 80: 185–197, 2003.
18. **Dickson AG, Sabine C, Christian JR.** Guide to best practices for ocean CO_2 measurements. *PICES Special Publication* 3: 1–191, 2007.
19. **Donaubauer HH.** Sodium- and potassium-activated adenosine triphosphatase in the excretory organs of *Sepia officinalis* (Cephalopoda). *Mar Biol* 63: 143–150, 1981.
20. **Dupont S, Havenhand J, Thorndyke W, Peck L, Thorndyke MC.** CO_2-driven ocean acidification radically affect larval survival and development in the brittlestar *Ophiothrix fragilis*. *Mar Ecol Prog Ser* 373: 285–294, 2008.
21. **Dupont S, Ortega-Martinez O, Thorndyke MC.** Impact of near-future ocean acidification on echinoderms. *Ecotoxycology* 19: 449–462, 2010.
22. **Dupont S, Thorndyke MC.** Impact of CO_2-driven ocean acidification on invertebrates early life history–what we know, what we need to know and what we can do. *Biogeosci* 6: 3109–3131, 2009.
23. **Evans DH, Piermarini PM, Choe KP.** The multifunctional fish gill: dominant site of gas exchange, osmoregulation, acid-base regulation, and excretion of nitrogenous waste. *Physiol Rev* 85: 97–177, 2005.
24. **Fabry VJ, Seibel BA, Feely RA, Orr JC.** Impacts of ocean acidification on marine fauna and ecosystem processes. *J Mar Sci* 65: 414–432, 2008.
25. **Febry R, Lutz P.** Energy partitioning in fish: the activity-related cost of osmoregulation in a euryhaline cichlid. *J Exp Biol* 128: 63–85, 1987.
26. **Feder ME, Walser JC.** The biological limitations of transcriptomics in elucidating stress and stress responses. *J Evol Biol* 18: 901–910, 2005.
27. **Feely RA, Sabine CL, Hernandez-Ayon JM, Ianson D, Hales B.** Evidence for upwelling of corrosive "acidified" water onto the continental shelf. *Science* 320: 1490–1492, 2008.
28. **Fioroni P.** Our recent knowledge of the development of the cuttlefish (*Sepia officinalis*). *Zool Anz* 224: 1–25, 1990.
29. **Fivelstad S, Olsen AB, Asgard T, Baeverfjord G, Rasmussen T, Vindheim T, Staffanson S.** Long-term sublethal effects on carbon dioxide on Atlantic salmon smolts (*Salmo solar* L.): ion regulation, haematology, element composition, nephrocalcinosis and growth parameters. *Aquaculture* 215: 301–319, 2003.
30. **Forsythe J, Lee P, Walsh L, Clark T.** The effects of crowding on growth of the European cuttlefish, *Sepia officinalis* Linnaeus, 1758 reared at two temperatures. *J Exp Mar Biol Ecol* 269: 173–185, 2002.
31. **Foss A, Rosnes BA, Oiestad V.** Graded environmental hypercapnia in juvenile spotted wolffish (*Anarhichas minor* Olafson): effects on growth, food conversion efficiency and nephrocalcinosis. *Aquaculture* 220: 607–617, 2003.
32. **Georgalis T, Perry SF, Gilmour KM.** The role of branchial carbonic anhydrase in acid-base regulation in rainbow trout (*Oncorhynchus mykiss*). *J Exp Biol* 209: 518–530, 2006.
33. **Gibbs A, Somero GN.** Na^+-K^+-adenosine triphosphatase activities in gills of marine teleost fishes: changes with depth, size and locomotory activity level. *Mar Biol* 106: 315–321, 1990.
34. **Gilmour KM, Perry SF.** Carbonic anhydrase and acid-base regulation in fish. *J Exp Biol* 212: 1647–1661, 2009.
35. **Gilmour KM, Thomas K, Esbaugh AJ, Perry SF.** Carbonic anhydrase expression and CO_2 excretion during early development in zebrafish *Danio rerio*. *J Exp Biol* 212: 3837–3845, 2009.
36. **Goyal S, Vanden Heuvel G, Aronson PS.** Renal expression of novel Na/H exchanger isoform NHE8. *Am J Physiol Renal Physiol* 284: F467–F473, 2003.
37. **Grigoriou P, Richardson CA.** Aspects of the growth of cultured cuttlefish *Sepia officinalis* (Linnaeus 1758). *Aquacult Res* 35: 1141–1148, 2004.
38. **Grigoriou P, Richardson CA.** The effect of ration size, temperature and body weight on specific dynamic action of the common cuttlefish *Sepia officinalis*. *Mar Biol* 154: 1085–1095, 2008.
39. **Grosell M.** Intestinal anion exchange in marine fish osmoregulation. *J Exp Biol* 209: 2813–2817, 2006.
40. **Gutowska MA, Melzner F.** Abiotic conditions in cephalopod (*Sepia officinalis*) eggs: embryonic development at low pH and high P_{CO_2}. *Mar Biol* 156: 515–519, 2009.
41. **Gutowska MA, Melzner F, Langenbuch M, Bock C, Claireaux G, Pörtner HO.** Acid-base regulatory ability of the cephalopod (*Sepia officinalis*) in response to environmental hypercapnia. *J Comp Physiol B* 180: 323–335, 2010.
42. **Gutowska MA, Melzner F, Pörtner HO, Meier S.** Cuttlebone calcification increases during exposure to elevated seawater P_{CO_2} in the cephalopod *Sepia officinalis*. *Mar Biol* 157: 1653–1663, 2010.
43. **Gutowska MA, Pörtner HO, Melzner F.** Growth and calcification in the cephalopod *Sepia officinalis* under elevated seawater P_{CO_2}. *Mar Ecol Prog Ser* 373: 303–309, 2008.
44. **Henry RP.** Multiple functions of carbonic anhydrase in the crustacean gill. *J Exp Zool* 248: 19–24, 1988.
45. **Henry RP, Cameron JN.** The role of carbonic anhydrase in respiration, ion regulation and acid-base balance in the aquatic crab *Callinectes sapidus* and the terrestrial crab *Gecarcinus lateralis*. *J Exp Biol* 103: 205–223, 1983.
46. **Henry RP, Swenson ER.** The distribution and physiological significance on carbonic anhydrase in vertebrate gas exchange organs. *Resp Physiol* 121: 1–12, 2000.
47. **Hoppema JMJ.** Carbon dioxide and oxygen disequilibrium in a tidal basin (Dutch wadden sea). *Neth J Sea Res* 31: 221–229, 1993.
48. **Horng JL, Lin LY, Huang JC, Katoh F, Kaneko T, Hwang PP.** Knockdown of V-ATPase subunit A (atp6v1a) impairs acid secretion and ion balance in zebrafish (*Danio rerio*). *Am J Physiol Regul Integr Comp Physiol* 292: R2068–R2076, 2007.
49. **Hu MY, Sucré E, Charmantier-Daures M, Charmantier G, Lucassen M, Melzner F.** Localization of ion regulatory epithelia in embryos and hatchlings of two cephalopods. *Cell Tiss Res* 441: 571–583, 2010.
50. **Hwang PP.** Ion uptake and acid secretion in zebrafish (*Danio rerio*). *J Exp Biol* 212: 1745–1752, 2009.
51. **Hwang PP, Lee TH.** New insights into fish ion regulation and mitochondrion-rich cells. *Comp Biochem Physiol A* 148: 479–497, 2007.
52. **Hyashi M, Kita J, Ishimatsu A.** Comparison of the acid-base responses to CO_2 and acidification in Japanese flounder (*Paralichthys olivaceus*). *Mar Poll Bull* 49: 1062–1065, 2004.
53. **Kimelberg HK, Papahadjopoulus D.** Phospholipid requirements for $(Na^+ + K^+)$ATPase activity: head-group specificity and fatty acid fluidity. *Biochim Biophys Acta* 282: 277–292, 1972.
54. **Kurihara H, Kato S, Ishimatsu A.** Effects of increased seawater P_{CO_2} on early development of the oyster *Crassostrea gigas*. *Aquat Biol* 1: 91–98, 2007.
55. **Kurihara H, Shimode S, Shirayama Y.** Effects of raised CO_2 concentration on the egg production rate and early development of two marine copepods (*Acartia steueri* and *Acartia erythraea*). *Mar Poll Bull* 49: 721–727, 2004.
56. **Kurihara H, Shirayama Y.** Effects of increased atmospheric CO_2 on sea urchin early development. *Mar Ecol Prog Ser* 274: 161–169, 2004.
57. **Lämmli UK.** Cleavage of structural proteins during the assembly of the head of Bacteriophage T4. *Nature* 227: 680–685, 1970.
58. **Larsen BK, Pörtner HO, Jensen FB.** Extra- and intracellular acid-base balance and ionic regulation in cod (*Gadus morhua*) during combined and isolated exposures to hypercapnia and copper. *Mar Biol* 128: 337–346, 1997.
59. **Lemaire J.** Table de développement embryonaire de *Sepia officinalis* L (Mollusque Céphalopode). *Bull Soc Zool Fr* 95: 773–782, 1970.
60. **Lewis E, Wallace DWR.** Program developed for CO_2 system calculations (ORNL/.CDIAC-105). Oak Ridge, TN: Oak Ridge National Laboratory, 1998.
61. **Marsh AG, Leong PKK, Manahan DT.** Gene expression and enzyme activities of the sodium pump during sea urchin development: implications for indices of physiological state. *Biol Bull* 199: 100–107, 2000.
62. **Mehrbach C, Culberso C, Hawley J, Pytkowic R.** Measurement of apparent dissociation constants of carbonic acid in seawter at atmospheric pressure. *Limnol Oceanogr* 18: 897–907, 1973.
63. **Melzner F, Göbel S, Langenbuch M, Gutowska MA, Pörtner HO, Lucassen M.** Swimming performance in Atlantic cod (*Gadus morhua*) following long-term (4–12 month) acclimation to elevated seawater P_{CO_2}. *Aqua Toxicol* 92: 30–37, 2009.
64. **Melzner F, Gutowska MA, Langenbuch M, Dupont S, Lucassen M, Thorndyke MC, Bleich M, Pörtner HO.** Physiological basis for high CO_2 tolerance in marine ectothermic animals: pre-adaptation through lifestyle and ontogeny? *Biogeosciences* 6: 2313–2331, 2009.
65. **Meunier B, De Visser SP, Shaik S.** Mechanism of oxidation reactions catalyzed by cytochrome P450 enzymes. *Chem Rev* 104: 3947–3980, 2004.

66. **Moyes CD, LeMoine CMR.** Control of muscle bioenergetic gene expression: implications for allometric scaling relationships of glycolytic and oxidative enzymes. *J Exp Biol* 208: 1601–1610, 2005.
67. **Palacios E, Racotta IS.** Salinity stress test and its relation to future performance and different physiological responses in shrimp postlarvae. *Aquaculture* 268: 123–135, 2007.
68. **Pane EF, Barry JP.** Extracellular acid-base regulation during short-term hypercapnia is effective in a shallow-water crab, but ineffective in a deep-sea crab. *Mar Ecol Prog Ser* 334: 1–9, 2007.
69. **Pecl GT, Steer MA, Hodgson KE.** The role of hatchling size in generating the intrinsic size-at-age variability of cephalopods: extending the Forsythe hypothesis. *Mar Freshw Res* 55: 387–394, 2004.
70. **Perry SF, Gilmour KM.** Acid-base balance and CO_2 excretion in fish: unanswered questions and emerging models. *Resp Physiol Neurobiol* 154: 199–215, 2006.
71. **Piermarini PM, Choi I, Boron WF.** Cloning and characterization of an electrogenic Na/HCO_3^- cotransporter from the squid giant fiber lobe. *Am J Physiol Cell Physiol* 292: C2023–C2045, 2007.
72. **Pörtner HO, Webber DM, Boutilier RG, O'Dor RK.** Acid-base regulation in exercising squid (*Illex illecebrosus*, *Loligo pealei*). *Am J Physiol Regul Integr Comp Physiol* 261: R239–R246, 1991.
73. **Pörtner HO, Langenbuch M, Reipschläger A.** Biological impact of elevated ocean CO_2 concentrations: lessons from animal physiology and earth history. *J Oceanograph* 60: 705–718, 2004.
74. **Ramnanan CJ, Storey KB.** Suppression of Na^+/K^+-ATPase activity during estivation in the land snail *Otala lactea*. *J Exp Biol* 209: 677–688, 2006.
75. **Schipp R, Mollenhauer S, Boletzky S.** Electron microscopical and histochemical studies of differentiation and function of the cephalopod gill (*Sepia officinalis* L.). *Zoomorph* 93: 193–207, 1979.
76. **Schwartz AA, Allen JC, Harigaya S.** Possible involvement of cardiac Na^+/K^+-adenosine triphosphatase in the mechanism of action of cardiac glycosides. *J Pharmacol Exp Ther* 168: 31–41, 1969.
77. **Seidelin M, Brauner CJ, Jensen FB, Madsen SS.** Vacuolar-Type H^+-ATPase and Na^+,K^+-ATPase expression in gills of Atlantic salmon (*Salmo salar*) during isolated and combined exposure to hypoxia and hypercapnia in fresh water. *Zool Sci* 18: 1199–1205, 2001.
78. **Somero GN, Childress JJ.** A violation of the metabolism-size scaling paradigm: activities of glycolytic enzymes in muscle increase in larger fish. *Physiol Zool* 53: 322–337, 1980.
79. **Spicer JI, Raffo A, Widdicombe S.** Influence of CO_2-related seawater acidification on extracellular acid-base balance in the velvet swimming crab *Necora puber*. *Mar Biol* 151: 1117–1125, 2007.
80. **Thomsen J, Gutowska MA, Saphörster J, Heinemann A, Trübenbach K, Fietzke J, Hiebenthal C, Eisenhauer A, Körtzinger A, Wahl M, Melzner F.** Calcifying invertebrates succeed in a naturally CO_2 enriched coastal habitat but are threatened by high levels of future acidification. *Biogeosciences* 7: 5119–5156, 2010.
81. **Toews DP, Holeton GF, Heisler N.** Regulation of the acid-base status during environmental hypercapnia in the marine teleost fish *Conger conger*. *J Exp Biol* 107: 9–20, 1983.
82. **Towle DW.** Sodium pump sites in teleost gill: unmasking by detergent (Abstract). *Am Zool* 177: 877, 1977.
83. **Tseng YC, Huang CJ, Chang JCH, Teng WY, Baba O, Fann MJ, Hwang PP.** Glycogen phosphorylase in glycogen-rich cells is involved in the energy supply for ion regulation in fish gill epithelia. *Am J Physiol Regul Integr Comp Physiol* 293: R482–R491, 2007.
84. **Turner N, Hulbert AJ, Else PL.** Sodium pump molecular activity and membrane lipid composition in two disparate ectotherms, and comparison with endotherms. *J Comp Physiol B* 175: 77–85, 2004.
85. **Virkki LV, Choi I, Davis BA, Boron WF.** Cloning of a Na^+-driven Cl/HCO_3^- exchanger from squid giant fiber lobe. *Am J Physiol Cell Physiol* 285: C771–C780, 2003.
86. **Wagner CA, Finberg KE, Breton S, Marshanski V, Brown D, Geibel JP.** Renal vacuolar-ATPase. *Physiol Rev* 84: 1263–1314, 2003.
87. **Wang T, Yang CL, Abbiati T, Schultheis PJ, Shull GE, Giebisch G, Aronson PS.** Mechanism of proximal tubule bicarbonate absorption in NHE3 null mice. *Am J Physiol Renal Physiol* 277: F298–F302, 1999.
88. **Yang TH, Somero G.** Activity of lactate dehydrogenase but not its concentration of messenger RNA increases with body size in barred sand bass, *Paralabrax nebulifer* (Teleostei). *Biol Bull* 191: 155–158, 1996.
89. **Young RE, Vecchione M.** Cephalopod gills. Tree of Life Web Project: http://www.tolweb.org/articles/?article_id=4200. 2004.

Corrigendum

Volume 69, May 2011

Hu MY, Tseng YC, Stumpp M, Gutowska MA, Kiko R, Lucassen M, Melzner F. Elevated seawater P_{CO_2} differentially affects branchial acid-base transporters over the course of development in the cephalopod *Sepia officinalis. Am J Physiol Regul Integr Comp Physiol* 300: R1100–R1114, 2011. First published February 9, 2011; doi:10.1152/ajpregu.00653.2010 (http://ajpregu.physiology.org/content/300/5/R1100).

Bankit numbers were listed in the text and Table 2 rather than GenBank accession numbers. In MATERIALS AND METHODS, section *Cloning of soNKA, soNBCe, soNDCBE, socCAII, and soV-AH Fragments*, the GenBank accession numbers are *NBC* (HM157263), *NDCBE* (HM157264), *CAII* (HM157265), and *VHA* (HM640218.1).

The following Table 2 lists the correct GenBank accession numbers for all genes.

Table 2. *Primer sequences used for qRT-PCR*

Gene Name	Abbreviation	Function	Acc. No.	Primer Sequence 5′-3′ (forward and reverse)	Amplicon Length
		Test Genes			
Na/K-ATPase	*NKA*	Electro/chemical gradient	GQ153672.1	CTGTCCTGAAAAGGGAATGCA TTTCCAATAGAAAGCTCAACACATTT	76
Na/HCO_3 cotransporter	*NBC*	Secondary active ion-transport	HM157263	GGAAGAATGCATGAAAGACACAAT TCGCTTCATGTGTTGATGGAA	70
Na-driven CI/HCO_3 exchanger	*NDCBE*	Secondary active ion-transport	HM157264	AGGAGCTGAATCCGCCAAT AGCCGGTAGCTTGGTGGTT	65
Carbonic anhydrase	*CA*	Bicarbonate formation	HM157265	ACCTTTAGCCATCCGCTGAA TCCGTTGTTGGTGACTTCCA	66
ATP-synthase	*ATP-Synth*	Electron transport chain	HM157266	GGAGAGAGCTGCCAAGATGAA CCTGGGTCTCGATGACTGGTA	74
Cytochrome p450	*CYP 450*	Xenobiotic defense	HM157268	CCGGCGGTGCCAGTTA TGCGGGAATTTTGTAATCATCA	69
Cytochrome-c oxydase	*COX*	Electron transport chain	YP514795	TCCTCCTCCGCAGTTGAAAG GCCCGCATGTGATAAGTTACTAGA	81
Octopine dehydrogenase	*ODH*	Anaerobic metabolism	AY545135	GCCGAGTCAACCCGGTTT CGCTGGTTCGACCTCCAA	65
		Reference Genes			
Cleavage and polyadenylation specificity factor	*CPSF*	mRNA polyadenylation	HM157279	CACACCAGCCCATGAAAAGA GGTGGTGTTGGCGAGTATGC	68
Ubiquitin-conjugated enzyme	*UBC*	Protein degradation	HM157280	CAATAATACCGTGAAAGTGGCAGAT TTTCCTGAGCTTCATATATTTCATCAG	74

Supplementary material to the manuscript entitled:

Elevated seawater pCO_2 differentially affects branchial acid-base transporters over the course of development in the cephalopod *Sepia officinalis*

Marian Y. Hu, Yung-Che Tseng, Meike Stumpp, Magdalena A. Gutowska, Rainer Kiko,

Magnus Lucassen, Frank Melzner

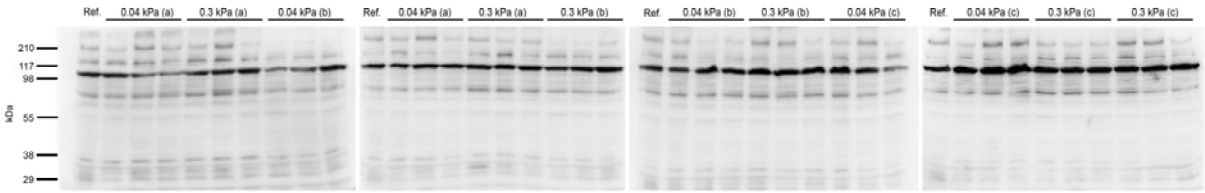

Fig. 1S. Quantification of Na^+/K^+-ATPase protein levels in control (0.04 kPa) and hypercapnia (0.3 kPa) treated animals for each time point (a = 48 h; b = 11 d; c = 42 d). Distinct immunoreactive bands were observed for Na^+/K^+-ATPase with a polyclonal antibody corresponding to the 100 kDa protein. A reference sample (Ref) was used to equalize signal intensities from different blots.

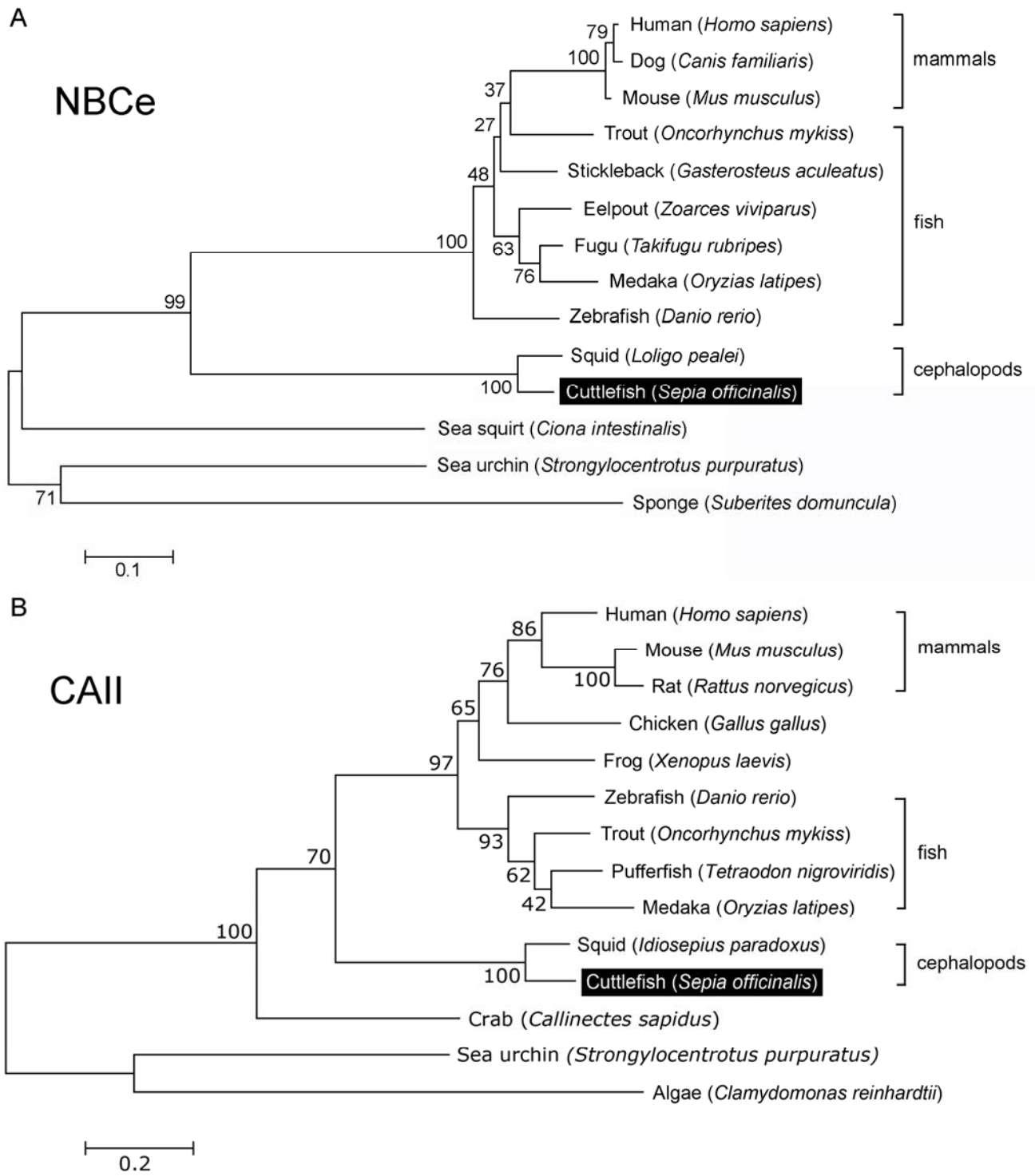

Fig. 2S. Phylogenetic tree obtained from amino acid sequences of the electrogenic Na^+/HCO_3^-cotransporter (NBCe) and carbonic anhydrase isoform 2 (CAII). Consensus trees were generated using the Neighbor-joining method with the pairwise deletion gap calculating option. The results were confirmed by 1,000 bootstraps. The unit of scale bar

is the number of amino acid substitutions per site. The cephalopods including cuttlefish (*S. officinalis*) squid (*L. pealei* and *I. paradoxus*) were compared to fish and mammals using lower marine invertebrates as an outgroup. The putative sequences of other species than *S. officinalis* were obtained from the NCBI and Ensembl databases as follows: *Homo sapiens* (NP_001091954.1), *Mus musculus* (NP_001129732.1), *Canis familiaris* (XP_850912.1), *Danio rerio* (EF634453.1), *Oncorhynchus mykiss* (AF434166.1), *Oryzias latipes* (ENSORLT00000003834), *Takifugu rubripes* (ENSTRUT00000039630), *Zoarces viviparus* (ACB46956.1), *Gasterosteus aculeatus* (ENSGACT00000019138), *Loligo pealei* (DQ469799.1), *Ciona intestinalis* (ENSCINT00000013690), *Strongylocentrotus purpuratus* (NM_001079551.1), *Suberites domuncula* (AJ628944.1). The GenBank accession numbers of the CAII sequences used as follows: *Homo sapiens* (NP_000058.1), *Mus musculus* (NP_033931.4) *Rattus norvegicus* (NP_062164.1), *Gallus gallus* (NP_990648.1), *Xenopus laevis* (NP_001080080.1), *Tetraodon nigroviridis* (GSTENG00025516001), *Idiosepius paradoxus* (DB918103), *Hydra magnipapillata* (XP_002165921.1), *Oryzias latipes* (ENSORLG00000012745), *Oncorhynchus mykiss* (NP_001117693.1), *Danio rerio* (NP_954685.1), *Chlamydomonas reinhardtii* (CAA38360.1), *Strongylocentrotus purpuratus* (XM_779235.2) and *Callinectes sapidus* (ABN51213) .

NBC and CAII Amino Acid Sequence Analysis

Phylogeny of *Sepia officinalis* so*NBCe*, as well as so*CAII* sequences were compared to electrogenic Na^+/HCO_3^+ co-transporters (*NBCe*) and cytosolic carbonic anhydrase isoform 2 (c*CAII*) amino acid sequence homologues obtained for mammals, fish, cephalopods and other invertebrates (Fig. 7).

S. officinalis NBC is most similar to squid sq*NBCe* indicated by a high boostrap value of 100%, but showing an outgroup topology to the orthologues of fish and mammals. Nevertheless, vertebrate and cephalopod *NBCe* sequences are closely grouped and supported by a high bootstrap value of 99% when using the amino acid sequence for electrogenic *NBC*e of invertebrates such as *Ciona intestinalis*, *Strongylocentrotus*

purpuratus and *Suberites domuncula* as an outgroup (Fig. 7A). Furthermore, phylogenetic relationships based on *cCAII* amino acid sequence confirm that *cCAII* orthologues of the three groups, mammals, fish and cephalopods are closely related when using the green algae *Clamydomonas reinhardtii* and the gram negative bacterium *Neissseiria gonorrhoeae* as an outgroup (Fig. 7B). The present sequence analysis suggests that the sequences for *NBCe* and *CAII* cloned in this study from cuttlefish gill are orthologues to those found in vertebrates.